

1

2 **A SENSITIVITY ANALYSIS APPLIED TO SPRAY AND CALPUFF MODELS WHEN**
3 **SIMULATING DISPERSION FROM INDUSTRIAL FIRES**

4

5 Francesca Tagliaferri ¹, Marzio Invernizzi¹, Laura Capelli ¹

6 ¹ *Politecnico di Milano, Department of Chemistry, Materials and Chemical Engineering “Giulio Natta” - P.za*
7 *Leonardo da Vinci 32, 20133 Milano, Italy*

8

9 * *Corresponding author: Marzio Invernizzi, marzio.invernizzi@polimi.it*

10

11 **HIGHLIGHTS**

- 12
- 13
- 14
- 15
- two atmospheric dispersion models are compared in terms of sensitivity to input data
 - SPRAY and CALPUFF sensitivities are generally comparable
 - the diameter is the parameter that determines the highest variability of the results
 - none of the “model specific parameters” leads to a significant output variation
- 16

17 **ABSTRACT:** This paper discusses a hypothetical case study in which SPRAY and CALPUFF dispersion models are
18 applied to the simulation of an incidental fire. For this type of accident, source features are typically not directly
19 measurable, thus making their definition critical. The choice of some model-specific parameters is another critical issue,
20 since clear indications are rarely available in guidelines. The aim of this work is to compare how pollutant concentrations
21 simulated with the two models are affected by changing these two sets of data (i.e. parameters related to the emission
22 source and model specific parameters), thus performing a sensitivity study to identify the most influential variables. The
23 most relevant outcome is that sensitivities of the two models are generally comparable, except for the source diameter: if
24 the SPRAY model is applied with the specific fire source option, then the concentrations result almost independent from
25 this parameter. Conversely, when considering other source-types, the concentrations vary up to +/- 60% within the
26 selected uncertainty range.

27 *Keywords: atmospheric dispersion modelling; sensitivity analysis; environmental impact; models comparison; source*
28 *characterization; fire simulation*

29 **1 INTRODUCTION**

30 At the very beginning of the oil industry, accidental fires were a matter of common occurrence, often
31 entailing disastrous effects at petroleum refining plants. Today, however, because of the development
32 of specific practices of fire prevention and extinguishing, fires are less frequent. Nonetheless, safety
33 measures cannot completely prevent this type of accidents (Shie and Chan, 2013; Sonnemans et al.,
34 2010). In addition, when they occur, they often have devastating consequences (Nivolianitou et al.,
35 2006; Zheng and Chen, 2011). First, in terms of economic losses: a small accident may cause million-

36 dollar property losses as well as some days of production interruption (Chang and Lin, 2006). The
37 second issue concerns the environmental damages caused by a fire on air quality, soil and water
38 (Langmann et al., 2009; Weichenthal et al., 2015). Indeed, the consequences on people's lives and
39 health is the matter of greatest concern (Griffiths et al., 2018).

40 The growing interest in monitoring air quality and assessing health risks makes the evaluation of the
41 consequences of a fire a key issue. Atmospheric dispersion models, which simulate the spatial
42 distribution of pollutants, represent an increasingly widespread tool for this type of evaluations
43 (Leelőssy et al., 2014). The use of numerical modelling in the field of industrial fire accidents has
44 become common nowadays, and this tendency is expected to increase with the continuous
45 improvement of the simulation tools.

46 Despite the growing number of applications of the modelling approach to evaluate the consequences
47 of fires (Adame et al., 2018; Henderson et al., 2008), on a regulatory level, precise guidelines
48 regarding the type of model and the setting of the model parameters are not available.

49 To perform a modelling study, input data relevant to the simulated domain (mapping, orography and
50 land use) and meteorological data are required. Furthermore, data concerning the emission scenarios
51 are needed, i.e. information concerning the emitted species (e.g., emission factors), the source
52 geometry, and its location in the domain. Finally, model-specific parameters, which are different
53 depending on the dispersion model used, must be implemented to perform the simulations.

54 Despite the great advantages associated with the use of dispersion models for atmospheric impact
55 assessment, there are still some important issues related to the uncertainty of these models (Chettouh
56 et al., 2014; Chutia et al., 2014; Russell and Dennis, 2000; Seibert, 2000). Accuracy of results
57 obtained from mathematical models is often hardly estimated, because of the presence of uncertainties
58 in the input data. Indeed, each of the input datasets represents a possible source of error (Holnicki and
59 Nahorski, 2015). In view of this, a sensitivity analysis is important to explore and quantify the impact
60 of possible changes in input data on the model outputs.

61 The aim of this paper is, based on a hypothetical case-study of a refinery fire, to discuss the sensitivity
62 of two dispersion models applied to simulate the dispersion of atmospheric pollutants, with the
63 purpose of investigating the most influential model input data.

64 As hypothetical case-study, we decided to consider a relatively small fire, involving a portion of gas
65 oil treatment unit. The reason for this choice is that the application of dispersion models is consistent
66 in such conditions, whereas for large catastrophic explosions the lack of representation of the
67 explosive phase or plume buoyancy in many models limits their application.

68 This work discusses the influence of possible errors in the source data and in model-specific
69 parameters on the results. The first objective is particularly interesting because of the high uncertainty
70 in the estimation of source term parameters for fires (Daly et al., 2012). Indeed, in the case of fires,
71 source geometrical features are hardly directly measurable, but they have to be estimated using
72 specific correlations. In our case study, the source term parameters (i.e. height, diameter and
73 temperature) were varied within a fairly limited range, since, as previously mentioned, we decided to
74 simulate a localized fire involving a single equipment.

75 Furthermore, the choice of some model-specific parameters is often critical, because clear indications
76 are rarely available in literature or in the specific model user's guides, and so their definition is
77 generally left to the professional judgement of the model user.

78 The work described in this paper uses two different approaches to assess the variability in the model
79 results. First, starting from a "base-case", defined as the most representative scenario for the case
80 study, different "plausible" emissive scenarios are investigated. Each of these scenarios is
81 characterised by a "macroscopic variation" of a single parameter within the hypothesized uncertainty
82 range. In this study, the term "macroscopic variation" refers to the extremes of the considered range
83 of variation of each parameter. The results obtained for each scenario are compared to the results of
84 the "base-case". This way, it is possible to evaluate the effect caused by a wrong estimation of an
85 input datum, which is crucially important especially in the case of environmental and health impact

86 assessments. This first approach allows to identify the most influential parameters on the model
87 outputs.

88 The second approach aims to further analyse the effect of these parameters by considering
89 “microscopic” variations thereof, i.e. a small Thus, this second investigation is intended to evaluate
90 effectively the model sensitivity to the different parameters, by imposing the same small percent
91 perturbation (compared to the reference base-case) to all, regardless of the reasonable range of
92 variability.

93 However, it should be highlighted that this paper does not aim to present an exhaustive numerical
94 sensitivity study. The adopted approach highlights the importance of having a broader view of the
95 issue relevant to the model sensitivity, thereby carrying out additional investigations focused on those
96 parameters that potentially generate the highest variations in the results.

97 It is worth noting that this sensitivity study has not been validated with experimental field
98 measurements, because it is a hypothetical event. Conversely, in real conditions, a model validation
99 is strongly suggested to evaluate the model accuracy and to select properly the reference base-case as
100 the most representative scenario.

101 For the purposes of the study, two models have been selected, i.e. the Lagrangian particle model
102 SPRAY and the puff model CALPUFF (Elbir, 2003; Elbir et al., 2010; Holnicki et al., 2016;
103 Rzeszutek, 2019). Indeed, Lagrangian particle models and puff models currently represent the most
104 common tools to simulate pollutants dispersion from fires (Adame et al., 2018; Ainslie and Jackson,
105 2009; Henderson et al., 2008). These models have been chosen because there is a large variety of
106 studies that prove their validity (Invernizzi et al., 2021), although, as previously mentioned, there are
107 no specific indications on a regulatory level.

108 It should be pointed out that the investigation of the most influential parameters cannot be generalized
109 to any model or to any situation, but it refers specifically to the selected case-study. This work does
110 not aim to suggest how to perform a sensitivity study applicable to any situation, nor addresses model

111 developers interested in developing or upgrading software. Actually, it highlights the importance of
112 investigating the possible range of variation of the input data to identify the most influential variables,
113 and it may represent a sort of guideline for model users who have to deal with the implementation of
114 similar case-studies.

115 Even though, in recent years, the use of dispersion models to simulate pollutant dispersion into the
116 atmosphere is continuously increasing, to the best of our knowledge, in literature there are few studies
117 relevant to model comparison in terms of sensitivity (Antonioni et al., 2012; Björnham et al., 2020;
118 Devenish et al., 2012; Gant et al., 2013; Srinivas et al., 2016). Also, the novelty of this work is related
119 to the approach followed to evaluate the model sensitivity. Indeed, the paper is not limited to
120 investigate the influence of the source term parameters on the model outputs, but it also considers
121 model-specific parameters. The latter are particularly interesting because for many of them, clear
122 indications on their setting are lacking both in the literature and in the model user's guides, thus
123 making it a critical issue for the modelist. Moreover, differently from other papers, this work proposes
124 a novel dual approach to address the issues that are relevant to the definition of the input data by
125 investigating the model sensitivity on two different levels.

126 **2 MATERIALS AND METHODS**

127 **2.1 Case – study description**

128 The hypothesized case study regards an incidental fire in an oil refinery: the event is supposed to
129 involve a portion of the gas oil treatment unit.

130 In our hypothesis, the fire lasts three hours. In real cases, the duration is a fundamental point to define
131 the case study and must be evaluated based on the statements of people who were on the spot.

132 To optimize the choice of the geographic simulation domain, the plume direction should be
133 considered. For the selected case study, a rectangular domain of 25x25 km has been identified with a
134 mesh grid of 250 m. Then, assuming that the plume evolves in south-western direction, the source
135 has been located at the north-eastern corner of the domain.

136 In addition, for a more precise analysis, some discrete receptors should be positioned in places
137 considered of particular interest to estimate the pollutants concentration resulting from the incidental
138 fire (e.g., hospitals, schools, city hall). In the identified scenario some receptors have been located as
139 to be representative of possible places of interest.

140 **2.2 Selection of the dispersion model**

141 A key element for an effective dispersion modelling study is to choose an appropriate modelling tool
142 to match the scale of impact and the complexity of the emission scenario. The choice of the most
143 suitable model can be based on the study of the scientific literature and the analysis of the technical
144 legislation, which are both useful in order to understand the features of each model.

145 The scientific literature is quite deficient in terms of studies concerning accidental fires in oil
146 refineries. Also, even though there are some studies comparing Lagrangian particle models and puff
147 models (Invernizzi et al., 2020; Ravina et al., 2020; Souto et al., 2001), to the best of our knowledge,
148 papers comparing their sensitivity to input data are lacking.

149 Nonetheless, there are several reviews (Holmes and Morawska, 2006; Leelóssy et al., 2014; Sinha et
150 al., 2004), which illustrate, in a rather comprehensive way, the different types of models that can be
151 used for the simulation of pollutants dispersion. Those reviews typically describe the model's features
152 and discuss advantages and disadvantages according to the kind of application.

153 In particular, according to the literature, Gaussian plume models (Islam, 1999; Liu et al., 2015),
154 Lagrangian puff models (Jung et al., 2003), Lagrangian particle models (Cécé et al., 2016; Santiago
155 and Martín, 2008), Eulerian grid models (Kota et al., 2013; Seland and Iversen, 1999) and fluid
156 dynamics models (Leelóssy et al., 2014; Markatos et al., 2009) may be used to simulate pollutants
157 dispersion. A detailed description of the different classes of dispersion models available is out of the
158 scope of this paper.

159 Here, some considerations have been made in order to choose the most suitable model for the selected
160 case study:

161 The greatest advantage of Gaussian models is that they have an extremely fast, almost
162 immediate, response time. However, the use of very simple models, such as Gaussians, is not
163 advisable in case of large simulation domains (Daly et al., 2012), because they consider steady
164 state conditions. Thus, they cannot adequately describe the dispersive phenomenon, since the
165 meteorological condition of one point of the domain is not representative of the wind field
166 variations over the entire domain.

- 167 • Eulerian and fluid dynamics models are very advanced simulators, but at the same time they
168 are very complex and require a long computational time.
- 169 • Fluid dynamics models are suggested, or even necessary, when the dispersion occurs in urban
170 areas, where the influence of buildings on the dispersion is dominant, or where the scale to
171 consider is the so-called meteorological microscale (<1 km) (Bhuiyan and Naser, 2015; Jang
172 et al., 2015; Mishra and Wehrstedt, 2015; Novozhilov, 2001). However, the considered case
173 study has a simulation domain larger than 1 km and the simulated site is not located in an
174 urban area, making such complex models unneeded.

175 For these reasons, a Lagrangian puff model (i.e. CALPUFF) and a Lagrangian particle model (i.e.
176 SPRAY) have been chosen: they represent a compromise between reasonable accuracy and
177 manageable computational time.

178 Furthermore, the use of these models for the selected case study is compliant with the Italian technical
179 standards on the matter (UNI 10796, 2009; UNI 10964, 2009). These standards define the scenarios
180 for the implementation of different models, suggesting the best model for each situation.

181 Finally, the available scientific literature also supports this choice: past studies prove the suitability
182 of these models in similar cases. For instance, there are some examples of studies carried out using
183 puff models, and specifically CALPUFF, for the simulation of pollutant dispersion from fires (Ainslie
184 and Jackson, 2009; Henderson et al., 2008).

185 On the other hand, there are fewer articles regarding the application of SPRAY to the simulation of
186 fires, presumably because it is a more recently developed model. However, the bibliographic research
187 proves the suitability of the Lagrangian models to simulate fires: the model behaviour is usually
188 compared with measured data to test its goodness, showing in most cases a good accuracy (Adame et
189 al., 2018; Liu et al., 2018).

190 **2.3 Meteorological and orographical features of the model**

191 The meteorological data used for the simulations are three-dimensional prognostic WRF data
192 purchased from Lakes Environmental. Each model processes the WRF data using the model-specific
193 meteorological tools (i.e. SWIFT for SPRAY and CALMET for CALPUFF), which are diagnostic
194 “mass consistent” models. They generate 3D wind fields inside the meteorological domain, which
195 has been set equal to the computational grid. For the simulations, the meteorological conditions were
196 chosen to be representative of a neutral winter morning with cloud cover.

197 The model also requires the site orography as input data. In this case, the simulated area is
198 characterized by a flat land.

199 **2.4 Definition of base-case**

200 Before starting a modelling study, it is necessary to quantify some parameters needed as input data.

201 In the case of a “real fire”, the first step is the quantification of the amount of fuel burnt. This can be
202 estimated by a mass balance around the involved equipment.

203 Then, for an incidental fire, the involved compounds and their emission factors shall be defined. The
204 scientific and technical literature states that the most common pollutants associated with gas oil
205 combustion are CO₂, CO, generic unburnt hydrocarbons (CH), particulate matter (PM), SO_x and NO_x
206 (Booher and Janke, 1997; Lemieux et al., 2004).

207 The SFPE Handbook of Fire Protection Engineering (DiNenno et al., 2002) has been chosen for the
208 estimation of emission factors, because it has been considered to be an authoritative and reliable

209 reference. More in detail, Table 3-4.14 “Yields of Fire Products and Chemical, Convective, and
210 Radiative Heats of Combustion for Well-Ventilated Fires” has been considered for the definition of
211 the emission factors of the CO₂, CO, unburnt hydrocarbons (CH) and particulate matter (PM) emitted
212 during the combustion of different fuels. Among all the listed species, the generic "Hydrocarbon" and
213 the kerosene have been considered, thus obtaining the following emission factors (ton/ton): 2.7 for
214 CO₂, 0.02 for CO, 0.007 for CH, and 0.05 for PM.

215 The SFPE Handbook of Fire Protection Engineering does not report emission factors for NO_x
216 emissions. Therefore, the emission factor for NO_x, which was set equal to 0.01 (ton/ton), was defined
217 using the AP-42 database of the US EPA, 1998..

218 For SO_x we assumed the complete (stoichiometric) conversion to SO₂ of the elemental sulphur (S) in
219 the original fuel, which was hypothesized to be 100 ppm, thus giving an emission factor of 0.002
220 (ton/ton).

221

222 The emission rate for each compound can be calculated as the product of its emission factor and the
223 amount of fuel burnt, divided by the event duration.

224 Furthermore, the model requires the geometrical features of the simulated source. Therefore, diameter
225 and height have to be evaluated from surveys and technical documentation.

226 In addition to the geometrical characterization of the source, some physical parameters have to be
227 defined. The fire smoke rise velocity is derived from the Ingason correlation (Ingason and Li, 2015):

228
$$w = \left(\frac{g \cdot q}{D/2 \cdot \rho_0 \cdot c_p \cdot T_a} \right)^{1/3} \quad (1)$$

229 where T_a is the ambient temperature, ρ_0 the air density, c_p the specific heat of air at constant pressure,
230 g is the acceleration of gravity, q the heat release and D the source diameter.

231 The Ingason correlation requires the estimation of the heat release, which may be derived from the
232 Babrauskas correlation (DiNenno et al., 2002):

233

$$q = m''_{\infty} \cdot \Delta h_{c,eff} (1 - \exp^{-(k\beta D)}) A \quad (2)$$

234 where $\Delta h_{c,eff}$ is the net heat of combustion, A is the source area, D is the diameter, and $k\beta$ and m''_{∞} are
 235 empirical constants available in literature for a number of common fuels. The values for the fuel of
 236 interest are obtained from DiNenno et al., 2002, Table 3-1.13 “Pool Burning: Thermochemical and
 237 Empirical Constants for a Number of Common Organic Fuels”, which reports the empirical constants
 238 for the most common organic fuels. Since specific data for gas oil are not available, the fuel that has
 239 been considered most representative among those listed is JP-5 ($\Delta h_{c,eff} = 43$ MJ/kg; $k\beta = 1.6m^{-1}$;
 240 $m''_{\infty} = 0.054$ kg/(m²s)).

241 Finally, it is necessary to define the fire temperature. To do this, the hydrocarbon fire curve, reported
 242 in BS EN 1363-2, 1999 showing the trend of the temperature as a function of time, has been used.

243 The maximum achievable temperature of about 1100 °C, has been considered for the hypothesized
 244 case study since it is rapidly achieved after a few minutes.

245 Based on these evaluations, a reference “base-case” was defined by setting the input parameters
 246 considered as most representative of the hypothesized emission scenario.

247 Its characteristic parameters are shown in Table 1:

248

249 **Table 1.** Source term parameters for the base-case. D = source diameter; T = plume temperature; H = source
 250 height; v = exit velocity; q = heat release; Quantity = amount of fuel burnt.

Scenario	D	T	H	v	q	Quantity	PM	CO	CO ₂	NO _x	SO ₂	HC
	[m]	[K]	[m]	[m/s]	[kW]	[ton]	[g/s]	[g/s]	[g/s]	[g/s]	[g/s]	[g/s]
BASE	5	1373	15	8.16	46354	11.2	51.8	20.7	2800	10.4	0.2	7.3

251

252 2.5 Source types and plume rise computation

253 One of the investigated parameters is the modelled source type. For both CALPUFF and SPRAY, the
254 fire is modelled by applying the specific source type suggested for fires (i.e. the buoyant area source
255 for CALPUFF, and the fire for SPRAY) and then compared with the model results obtained by
256 assimilating the fire to a point source (i.e. stack).

257 According to the CALPUFF User's Guide (Scire et al., 2000), the buoyant area source is the most
258 appropriate tool to simulate fires. Therefore, for the CALPUFF simulations, the point source has been
259 considered only for the "base-case", because of its unsuitability to model the selected event. Despite
260 the indications of the User's Guide, the point source has been implemented in the CALPUFF "base-
261 case" to highlight the differences in the ground concentrations in comparison to the buoyant area
262 source, as will be discussed in Paragraph 3.1, and, consequently, to underline the importance of using
263 the specific fire options available in the models.

264 For each type of source, the dispersion model simulates the plume rise mechanism according to a
265 different scheme. When considering the fire as a point source (without any fire-specific option), both
266 CALPUFF and SPRAY calculate the buoyancy flux according to the Briggs equation (Tinarelli,
267 2017), which is proportional to the square of the source radius:

$$268 \qquad F_b = gr^2w_0 \frac{T-T_a}{T_a} \qquad (3)$$

269 where g is the acceleration of gravity, r the source radius, w_0 the effluent exit velocity, T_a the ambient
270 temperature and T the exit smoke temperature.

271 When using the CALPUFF - buoyant area source model, the radiative heat loss from the plume to the
272 ambient air can be estimated using the following equation (Scire et al., 2000):

$$273 \qquad \frac{q}{c_p} r^2 = -2\varepsilon\sigma r(T^4 - T_a^4)/c_p \qquad (4)$$

274 where q is the radiative heat loss, c_p the specific heat of the ambient air, r the source radius, σ the
275 Stefan-Boltzmann constant, ε the emissivity, T the plume temperature and T_a the ambient

276 temperature. Here, an increase of the radius implies a reduction of the heat losses. Consequently, the
277 plume rise increases and the pollutant concentrations decrease.

278 On the other hand, if the SPRAY model is used in combination with the specific fire option, the
279 equation used for the buoyancy calculation, in which neither velocity nor radius appear, results in a
280 buoyancy flux not affected by the source diameter (Tinarelli, 2017):

$$281 \quad F_b = \frac{gP}{\pi c_p \rho_{air} T_a} \varepsilon \quad (5)$$

282 where $\varepsilon = 0.7$ represents the reduction term due to radiation, P is the energy/time, g the acceleration
283 of gravity, c_p and ρ_{air} the specific heat and the density of the ambient air, and T_a is the ambient
284 temperature.

285 **2.6 Definition of alternative cases for the evaluation of the effects of source** 286 **characterization**

287 Starting from the “base-case”, it has been decided to investigate alternative emission scenarios by
288 changing the most critical geometrical parameters of the source within a reasonable range of variation.
289 Indeed, the estimation of these variables is characterized by high uncertainty because of the
290 impossibility of measuring them directly during the event.

291 In addition to the source geometrical parameters, other variables associated with the definition of the
292 emission scenario have been investigated (e.g., temperature and amount of fuel burnt).

293 Under real conditions of a refinery fire, in order to define the alternative scenarios, it is advisable to
294 first validate the base-case, with the purpose to verify that this is effectively the most representative
295 and realistic scenario. However, it shall be considered that this is usually very complex in case of
296 accidental fires.

297 The alternative scenarios defined for the study are shown in Table 2, with the numbers in bold
298 representing the variables changed in the alternative scenarios.

299 **Table 2.** Alternative scenarios for the source term parameters

Scenario	D	T	H	v	Quantity	PM	CO	CO ₂	NO _x	SO ₂	HC
	[m]	[K]	[m]	[m/s]	[ton]	[g/s]	[g/s]	[g/s]	[g/s]	[g/s]	[g/s]
A1	10	1373	15	6.21	11.2	51.852	20.741	2800	10.37	0.207	7.259
A2	3.5	1373	15	9.17	11.2	51.852	20.741	2800	10.37	0.207	7.259
H1	5	1373	20	8.16	11.2	51.852	20.741	2800	10.37	0.207	7.259
T1	5	1273	15	8.16	11.2	51.852	20.741	2800	10.37	0.207	7.259
T2	5	1473	15	8.16	11.2	51.852	20.741	2800	10.37	0.207	7.259
Q2	5	1373	15	10.28	22.4	103.703	41.481	5600	20.74	0.4148	14.518
Q2A1	10	1373	15	7.86	22.4	103.703	41.481	5600	20.74	0.4148	14.518
Q5A1	10	1373	15	10.68	56.0	259.260	103.71	14000	51.85	1.035	36.295

300

301 It is worth underlining that, when using the SPRAY - fire model, scenarios T1 and T2 have not been
302 considered, since the fire temperature is not an input parameter required by the software.

303 2.7 Evaluation of the effects of model-specific parameters

304 2.7.1 CALPUFF

305 As far as CALPUFF is concerned, the only model-specific parameter that has been investigated is the
306 initial vertical dispersion coefficient σ_{z0} , which defines the initial dimension of the puff in the vertical
307 direction. Concerning the base-case scenario, as suggested in the user's guide for Gaussian plume
308 models (US EPA, 1995), σ_{z0} is evaluated as follows:

$$309 \sigma_{z0} = H/2.15 \quad (6)$$

310 where H is the source height.

311 This correlation is recommended for surface-based sources, as it is the case in the modelled case-
312 study.

313 However, in literature, other correlations are reported, which can be adopted depending on the source
314 elevation or the presence of adjacent buildings. More in detail, in case of elevated source located on

315 or adjacent to a building, it is suggested to divide the building height by a factor of 2.15. In case of
316 an elevated source not adjacent to a building, it is recommended to divide the vertical dimension of
317 the source by 4.3 (US EPA, 1995). Accordingly, to run the alternative scenario, σ_{z0} is set equal to the
318 source height divided by 4.3.

319 **2.7.2 SPRAY**

320 SPRAY is a more advanced software: it requires the definition of several parameters, whose
321 estimation is not trivial, due to the absence of specific indications.

322 **2.7.2.1 Height of the first layer**

323 Differently from CALPUFF, which provides the output concentration in a gridded surface at the
324 ground, the Lagrangian particle model needs the *height of the first layer* as input datum: it is the
325 height of the first cell above ground used by the model to compute the concentration in any point
326 $P(x;y;z;t)$ at time t . To do this, the model computes the pollutant concentration considering a
327 “sampling volume” having the grid step dimensions in x and y direction, and the third dimension z
328 is the *height of the first layer*.

329 The value attributed to this parameter for the base-case is 10 m: on one hand, in order to evaluate the
330 ground level concentration, the first layer height should be sufficiently low and, on the other hand, a
331 too low value is not advisable in order to limit the
332 influence of the mechanical turbulence, the effect of which is more pronounced in the vicinity of the
333 terrain, progressively decreasing moving far from the ground.

334 In addition, the surface roughness shall be considered for the evaluation of this parameter. The
335 roughness length z_0 represents the height where the wind speed becomes zero (no-slip condition) and
336 it is related to the terrain features: depending on the land use type, different values for z_0 are suggested.
337 In particular, in case of urban areas, SPRAY (ARIANET, 2011) sets this parameter to 1 m. Hanna

338 and Britter (2002) suggested that the ratio between z_0 and the obstacle height H_r can be estimated
339 according to a simple rule of thumb:

340
$$\frac{z_0}{H_r} = 0.1 \quad (7)$$

341 It follows that the parameter H_r assumes a value of 10 m. Also, Hanna and Britter (2002) highlighted
342 that for a typical urban or industrial site an average building height of 10 m is a reasonable estimation.
343 Since one of the main purposes of an atmospheric dispersion model is the assessment of the impact
344 on people, it is reasonable to consider the height up to which the concentration estimation is of interest
345 (i.e. the height of the first layer) of 10 m.

346 **2.7.2.2 Δz**

347 Another model-specific parameter that has to be defined is Δz , i.e. the vertical dimension of the
348 “emission parallelepiped”. SPRAY generates particles uniformly distributed on a “terrain following”
349 parallelepiped centred in P (X_0 , Y_0 , Z_0), which are the coordinates of the emission region centre of
350 gravity, the vertical dimension of which is Δz (Tinarelli, 2017).

351 In other words, this parallelepiped can be thought of as a box in which the particles initially appear.
352 Thus, they are released in a vertical region ranging from $Z_0 - \Delta z/2$ and $Z_0 + \Delta z/2$, with Z_0 coincident
353 with the source height. In the Supplementary Material S1 a sketch of the emission parallelepiped is
354 shown, highlighting its vertical dimension Δz , and its position with respect to the emission source.

355 This variable describes the initial condition of the emission and it should be defined as to reproduce
356 the geometrical features of the emission region. The “geometrical features of the emission region”
357 refers not only to the effective source dimensions, but also to the dynamic effects affecting the
358 emission. For instance, because of the configuration of the stack or of the adjacent buildings, the
359 plume may not rise freely in the atmosphere: some aerodynamic effects due to the way the wind
360 moves around adjacent buildings and the stack can force the plume towards the ground instead of
361 allowing it to rise. Depending on the stack height, it may be possible for the plume to be pulled down

362 into this wake area (*building downwash*) resulting in high concentrations immediately downwind of
363 the source. Therefore, to reproduce the emission region, a conservative value equal to twice the source
364 height (30 m) has been defined.

365 **2.7.2.3 Number of particles**

366 Another investigated parameter is related to the stochastic description of the Lagrangian model. The
367 air is described as a set of parcels that move according to two different mechanisms: advection and
368 turbulent motion. The irregular and highly variable nature of the main parameters describing the
369 motion of a molecule in the air makes it not possible to use exact values of them in any practical
370 problem, since a fully deterministic approach is almost impossible.

371 The SPRAY model requires the definition of the number of particles used for the simulations;
372 whereby each particle represents a discrete amount of pollutant. For this variable, a suitable value has
373 been selected in retrospect, after running some simulations with different numbers of particles. To
374 identify a reasonable value, a compromise between good accuracy in the results and manageable
375 computational time has been considered, leading to a choice of about 3 million of particles emitted in
376 the three hours of simulation. To ensure a detailed description of the particles motion, a sufficiently
377 high number of particles is required. Indeed, the smaller the sample size is, the more *outliers* may
378 skew the findings. In other words, the particles represent the air parcels. Thus, each particle has a
379 random contribution of motion that has to be described considering a stochastic approach. If the
380 particles number is high enough, an average behaviour can be identified, minimizing the discrete
381 contribution of each particle. Conversely, if few particles are considered, there is the risk that the
382 *outliers* are heavier. In other words, the number of particles should be high enough as to ensure that
383 the results do not show any statistically meaningful difference when changing this variable.

384

385 Table 3 shows the model-specific parameters for SPRAY and CALPUFF selected for the base-case
 386 and the alternative scenarios, with the numbers in bold representing the variables changed in the
 387 alternative scenarios.

388 In order to investigate the effect of the particles number, the case with the highest number of particles
 389 (i.e. 74'682'000 particles emitted in three hours, from the SPRAY default release option of 34575
 390 particles in 5 seconds) has been considered as a reference, whereas the "base-case" with 2'989'440
 391 particles is treated as an alternative scenario. This is the reason why, in Table 3, the scenario with
 392 74'682'000 is not reported, because it is considered as the reference scenario to compute the
 393 sensitivity of the results with respect to the number of particles in the alternative scenarios
 394 (PARTICLE1 - PARTICLE8)

395 **Table 3.** SPRAY and CALPUFF model specific parameters for *base-case* and alternative scenarios

SPRAY				CALPUFF	
Scenario	Δz [m]	H_1° Layer [m]	Particle number	Scenario	σ_{z0} [m]
BASE	30	10	2'989'440	BASE	6.98 (=H/2.15)
Δz_2	15	10	2'989'440	$\sigma_{z0,1}$	3.49 (=H/4.3)
Δz_3	20	10	2'989'440		
Δz_4	25	10	2'989'440		
H_1L	30	4	2'989'440		
PARTICLE1	30	10	151'200		
PARTICLE2	30	10	749'520		
PARTICLE3	30	10	2'492'640		
PARTICLE4	30	10	2'989'440		
PARTICLE5	30	10	7'471'440		
PARTICLE6	30	10	10'670'400		
PARTICLE7	30	10	14'938'560		
PARTICLE8	30	10	24'896'160		

396

397 2.8 Sensitivity analysis

398 Once the most influential parameters have been identified by means of the simulations relevant to the
399 alternative scenarios, a sensitivity analysis is needed in order to quantify the effects of a “microscopic
400 variation” of the input variables on the model outputs.

401 2.8.1 Choice of the approach

402 The choice of the method to be used for the sensitivity analysis was based on a deep literature search.
403 As a result, a paper proposing a sensitivity analysis based on the Taylor series approach by Yegnan
404 et al. (2002) has been selected, because it well-suits the hypothesized case-study.

405 Indeed, Yegnan et al. (2002) adopted this approach to calculate the sensitivity of ground level
406 concentrations resulting from a short-term simulation (one hour), as in the case of four hypothesis.
407 Also, after the definition of a “base-case” for the modelling scenario, each of the seven input
408 parameters (many of which are the same investigated in the alternative scenarios reported in Table 2,
409 e.g., stack height, stack diameter, temperature) has been modified to determine the ones that mostly
410 affect the output concentrations, i.e. the parameters to which the model is most sensitive.

411 In the paper by Yegnan et al. (2002), the “base-case” identified is the most representative scenario
412 the average values are derived from. Then, the most sensitive input parameters, i.e. wind speed and
413 temperature, are perturbed by 1% in both directions with respect to the average values, and the
414 corresponding change in the output is evaluated. The sensitivity of the output $f(x)$ is then computed
415 as:

$$416 \qquad f'(\bar{x}) = \frac{f(x_2) - f(x_1)}{x_2 - x_1} \qquad (8)$$

417 where \bar{x} is the value of the input parameter adopted in the reference base-case, x_1 and x_2 are the
418 perturbed input values on either side of \bar{x} , and $f(x_1)$ and $f(x_2)$ are the corresponding output values.

419 Also, to normalize the results by removing the effects of units, the dimensionless sensitivity index
420 (Gonsamo, 2011; Rodrigues et al., 2013) is introduced:

$$421 \quad f'(\bar{x})^N = f'(\bar{x}) \cdot \frac{\bar{x}}{\bar{y}} \quad (9)$$

422 where the apex N refers to the normalization of the sensitivity index, and \bar{y} is the value of the output
423 resulting from the reference base-case (with \bar{x} as input variable).

424 Rodrigues et al., (2013) defined the normalized sensitivity index of a variable with respect to a
425 parameter as “the ratio of the relative change in the variable to the relative change in the parameter”.
426 Thus, it is obtained by multiplying $f'(\bar{x})$ by the ratio of the parameter value to the model result for
427 the *base-case* scenario.

428 **2.8.2 Application of the method to the case study**

429 To perform the sensitivity study discussed in the previous paragraph, the investigated parameters
430 have been perturbed by 1%, 2% and 3% in both directions with respect to the value of the *base-case*,
431 while all the other parameters were kept unchanged.

432 Then, the concentration values resulting from these perturbations have to be computed on a set of
433 discrete receptors. In this case, 40 receptors placed along the plume axis starting from the source and
434 spaced 250 m from each other were considered.

435 This sensitivity study has a different purpose compared to the approach based on the evaluation of
436 the alternative scenarios. In this case, the perturbations imposed to the investigated variables are not
437 the extremes of a reasonable range of variability for the selected parameter, but a “microscopic”
438 perturbation is considered. As a result, the sensitivity analysis is intended to evaluate the numerical
439 model sensitivity to the investigated variables, regardless of the range of variability thereof.

440 In particular, this approach allows to:

- 441 ▪ Compare effectively the model sensitivity to different parameters, by imposing the same
442 perturbations to all of them;

- 443 ▪ Investigate the model behaviour caused by a perturbation of the selected parameter,
444 identifying, for instance, the relationship existing between the input and the output;
- 445 ▪ Identify the way the model sensitivity to the selected parameter changes if moving far from
446 the source;
- 447 ▪ Compare SPRAY and CALPUFF sensitivity to the selected parameters, highlighting which
448 of them is more sensitive to perturbations of the investigated input data.

449 One important preliminary consideration concerns the applicability of this approach to the SPRAY
450 model, whereby the number of particles may affect the significance of the calculated sensitivity
451 indexes. Indeed, to obtain reliable results from this test, since the variation applied to the parameters
452 is significantly low (i.e. 1%-3%), it is important to reduce as much as possible the influence related
453 to the choice of the number of particles.

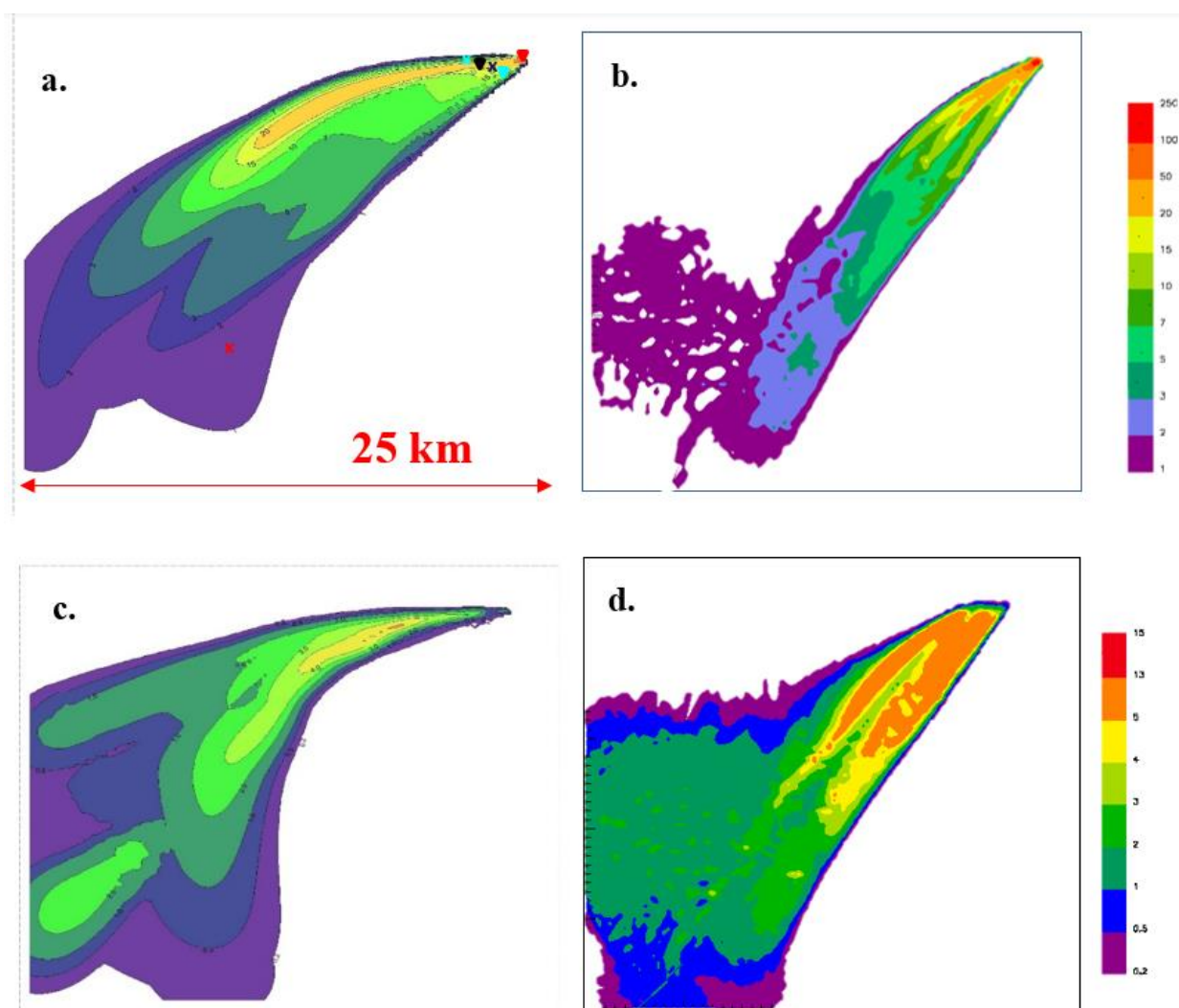
454 For this reason, it is necessary to adopt a significantly high number of particles to run these
455 simulations. For the selected case-study, Supplementary Material S2 shows that simulations with
456 106'688'880 particles have negligible variability due to the number of particles. For this reason, the
457 sensitivity analysis for the SPRAY model is carried out considering the emission of 106'688'880
458 particles.

459 **3 RESULTS AND CRITICAL DISCUSSION**

460 **3.1 Results of “base-case” for different source types**

461 The simulation results can be processed with the post processing tools of each of the models under
462 investigation (i.e. CALPOST for CALPUFF and POSTBIN for SPRAY). This way, ground level
463 concentration maps representing the pollutants dispersion within the simulation domain are
464 obtained. As an example of the simulation results, Figure 1 shows the maximum 1-hour
465 concentration maps for the PM resulting from the *base-case* simulation in function of the different

466 source types explained in section 2.5. The simulation of PM dispersion has been run as for an
 467 inert gas (no deposition considered). PM was selected as the “tracer” to be treated as reference
 468 species for further evaluations, since it is, among the compounds considered, the one with the
 469 highest emission rate after CO₂. Therefore, from this point forward, PM will be referred to as
 470 “Tracer”. It should be highlighted that the reference compound chosen doesn’t affect the
 471 forthcoming considerations about model sensitivity or the comparison between different source
 472 types: the same considerations could be applied to any other species considered.



473
 474 **Figure 1.** Maximum ground level concentration maps of the tracer species resulting from CALPUFF-buoyant area (a.),
 475 SPRAY- fire (b.), CALPUFF-point (c.) and SPRAY-point (d.). Figure (a.) shows the position of the six discrete
 476 receptors discussed below: \blacktriangledown = R_1, x =R_2, \blacktriangleleft = R_3, x =R_4, \blacktriangledown = R_5, x =R_6.

477 Depending on the source type and the dispersion model used, slightly different plume directions can
 478 be observed. The maps in Figure 1 differ in concentration and plume shapes: this can be explained

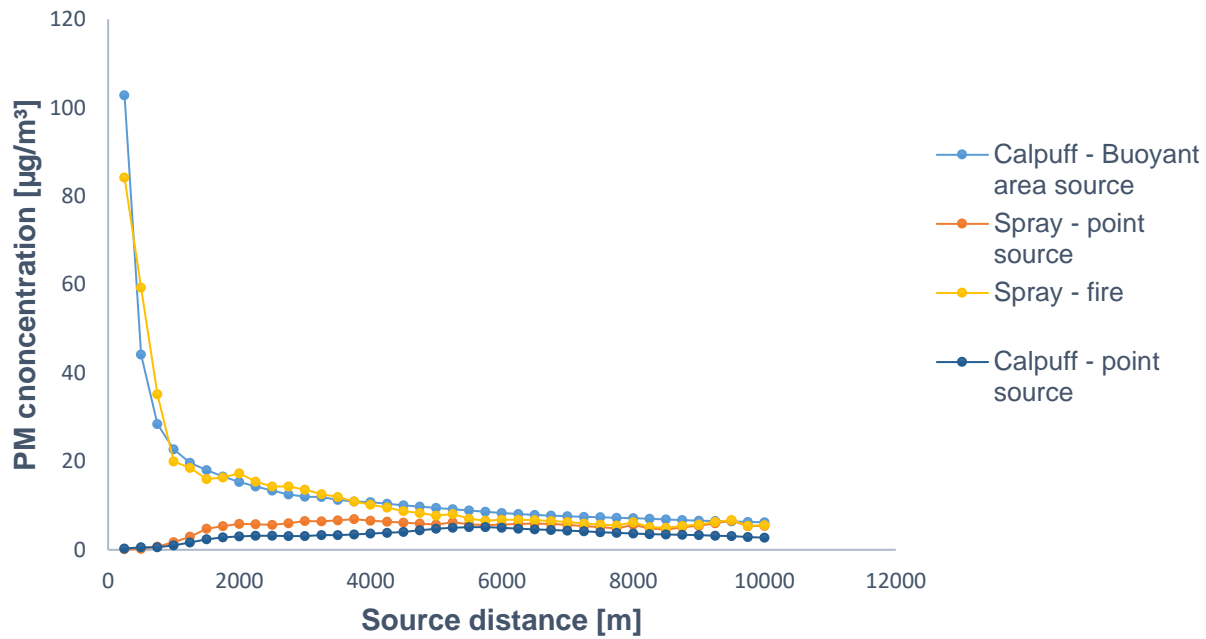
479 considering the different wind fields resulting from the application of the different met pre-
 480 processors. Indeed, despite starting from the same raw meteorological input data, the different
 481 meteorological pre-processors (i.e. CALMET for CALPUFF and SWIFT for SPRAY) elaborate the
 482 results in a slightly different way. As an example, the picture of the wind field computed by CALMET
 483 and SWIFT for the same hour is reported in the Supplementary Material S3.

484 The maximum Tracer concentrations calculated by the models on a set of selected discrete receptors
 485 (indicated in Figure 1(a.)) are reported in Table 4. More in detail, receptor 1 corresponds to the
 486 gridded receptor where the maximum concentration has been calculated by the two models inside the
 487 simulation domain, receptors (2-5) are representative of places of public interest and receptor 6 is the
 488 point of maximum concentration at the plant fence line.

489 **Table 4.** Maximum Tracer concentration values at selected receptors calculated by CALPUFF (left) and SPRAY
 490 (right)

ID	Description	CALPUFF		SPRAY	
		Conc. (point source) [$\mu\text{g}/\text{m}^3$]	Conc. (buoyant area) [$\mu\text{g}/\text{m}^3$]	Conc. (point source) [$\mu\text{g}/\text{m}^3$]	Conc. (fire) [$\mu\text{g}/\text{m}^3$]
R_1	MAX DOMAIN	5.12	114.48	12.97	213.2
R_2	RANK 1 SENSITIVE	0.77	1.05	4.19	4.99
R_3	RANK 2 SENSITIVE	0.23	14.69	4.28	23.6
R_4	RANK 3 SENSITIVE	2.44	11.46	5.67	19.45
R_5	RANK 4 SENSITIVE	3.78	18.83	5.60	22.87
R_6	MAX FENCELINE	0.31	19.29	6.64	23.31

491
 492 Figure 2 shows the trend of the of maximum 1-hour concentration of the Tracer as a function of the
 493 distance from the source. To the purpose, 40 receptors placed along the plume axis starting from the
 494 source and spaced 250 m from each other are considered.



495 **Figure 2.** Maximum Tracer concentration trend in function of the source distance for the different combinations of
 496 dispersion models and source types considered
 497
 498

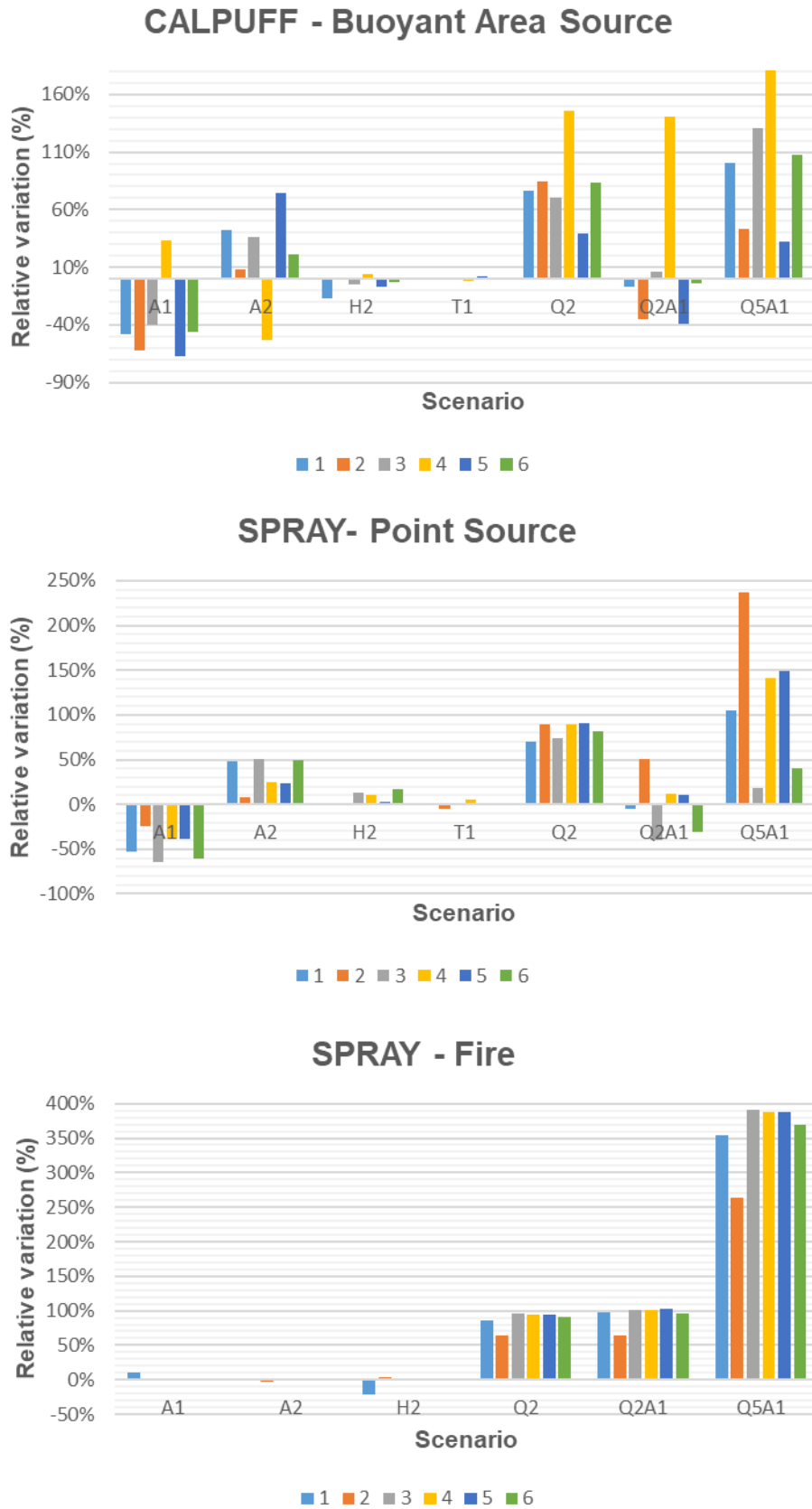
499 The different trends shown in Figure 2 can be explained by considering the different plume rise
 500 computations for point sources and for fires/buoyant area sources. According to the SPRAY model
 501 for fires, which considers a non-complete combustion, there is a cold fraction of particles that remains
 502 unburnt and immediately falls to the ground, without being dragged into the plume rise. This gives
 503 the highest Tracer concentrations close to the source. As far as CALPUFF is concerned, the buoyant
 504 area source model considers radiative heat losses due to the high plume temperature near the burning
 505 source. Consequently, the heat flux along the plume trajectory will be reduced, leading to a lower
 506 buoyancy flux. On the contrary, for point sources, the maximized plume rise leads to very low
 507 concentration values close to the emission point, whereas a concentration peak is observed at the
 508 distance where the plume reaches the ground.

509 At high distance from the source (>5000m) the maximum Tracer concentrations computed by the
 510 different models tend to become very similar, giving concentrations ranging from 5 to 9 $\mu\text{g m}^{-3}$ at
 511 5000 m from the source and from 3 to 6 $\mu\text{g m}^{-3}$ at 10000 m from the source.

512

513 **3.2 Alternative scenarios for source geometrical features and emission scenario**
514 **characteristics**

515 Figure 3 shows, for the different source types, the variability (%) of the maximum Tracer
516 concentration values resulting at the selected receptors 1-6 (which are the same as for the base-case,
517 which are reported in Table 4) from the simulations relevant to the alternative scenarios were
518 compared to those obtained for the base-case. It is worth recalling that, for reasons discussed in
519 Section 2.5, the point source simulated by CALPUFF will not be considered from this moment on.



520
521
522

Figure 3. % variation of the maximum PM concentration values at the selected receptors resulting from the simulations of the alternative emission scenarios compared to the reference base-case for the different source types

523 This investigation shows that the diameter of the source is one of the most interesting source term
 524 parameters, because of its different influence on the model outputs depending on the considered
 525 source type: it significantly affects the model outputs when using the CALPUFF - buoyant area source
 526 model or the SPRAY - point source model, but it leads to very low variations when applying the
 527 SPRAY model in combination with the specific fire option. Thus, to examine the source diameter
 528 influence more deeply, Table 5 reports the relative variation (%) relevant to the scenarios A1 and A2,
 529 where only the geometric dimension of the source has been modified if compared to the base case.

530 **Table 5.** % variation of the maximum Tracer concentration values at the selected receptors resulting from the A1
 531 and A2 scenarios compared to the reference base-case for the different combinations of models and source types
 532 considered

ID	CALPUFF (Buoyant Area)		SPRAY (Point)		SPRAY (Fire)	
	A1	A2	A1	A2	A1	A2
1	-48.10%	42.10%	-52.40%	47.60%	10.20%	-0.80%
2	-61.90%	7.60%	-24.80%	8.10%	2.00%	-2.40%
3	-40.50%	35.70%	-64.50%	50.90%	2.50%	0.20%
4	32.90%	-53.30%	-39.00%	24.70%	2.10%	1.00%
5	-67.10%	74.40%	-38.60%	23.20%	1.10%	0.30%
6	-45.70%	21.00%	-59.90%	49.90%	1.30%	0.30%

533

534 Considering CALPUFF and the point source simulated by SPRAY, the simulations conducted at the
 535 boundaries of the uncertainty range for the source diameter result in significant variations in the
 536 maximum modelled Tracer concentrations at selected receptors. A decrease of the diameter from 5 m
 537 to 3.5 m (scenario A2) generally results in an increase of the simulated maximum Tracer
 538 concentrations of about 50%, whereas an opposite effect is obtained by increasing the diameter from
 539 5 m to 10 m (scenario A1), generally giving decreased concentrations of about 60%. On the other
 540 hand, when using the SPRAY – fire model, the source diameter does not represent a highly influential
 541 variable, giving a maximum variability of 10% at the selected receptors.

542 When using the SPRAY - point source model, the effect of the source can be explained by considering
 543 the buoyancy flux computation, performed according to the Briggs equation (see Section 2.5).

544 The source diameter affects the buoyancy of the plume indirectly through the radius and the exit
545 velocity, which are required to calculate the buoyancy flux. More in detail, the diameter has an
546 opposite effect on these two parameters (see Section 2.5). An increase in the diameter means a small
547 decrease in the velocity whereas the source radius, which is squared in the Briggs equation, increases
548 significantly. Therefore, the dominant term is the second one, leading to an increased buoyancy flux
549 and a reduction in the ground level concentrations.

550 When using the CALPUFF - buoyant area source model, the computation of the radiative heat loss
551 from the plume to the ambient air depends on the source radius. Here, an increase of the radius implies
552 a reduction of the heat losses. Consequently, the plume rise increases and the pollutant concentrations
553 decrease.

554 On the other hand, if the SPRAY model is used in combination with the specific fire option, the
555 influence of the diameter of the source on the model outputs turns out to be negligible. From a
556 mathematical point of view, this can be explained by the equation used (see Section 2.5) for the
557 calculation of buoyancy flux, where neither velocity nor radius appear, giving that the buoyancy
558 calculation is not affected by the source diameter.

559 The second investigated parameter is the source height, the influence of which on the model output,
560 (Figure 3), is less relevant: for all the investigated sources, the variability has the same order of
561 magnitude and it does not significantly affect the model results. Also, depending on the position of
562 the selected receptor, it may lead to an increase or a decrease in the maximum Tracer concentration,
563 but in all cases the variabilities (%) are significantly lower than those produced by the variation of
564 the source diameter. The same consideration applies to the model sensitivity to temperature. Its
565 influence on the concentration values is even lower, giving a maximum variation on the selected
566 receptors of 5% (Figure 3).

567 In the Q2 scenario (Figure 3), where the amount of fuel burnt is doubled compared to the reference
568 scenario, the resulting concentration at the receptors is not doubled, as the calculated variability is

569 always lower than 100%. The explanation for this behaviour is that, at constant diameter, by
570 increasing the fuel burnt, the heat released by the fire increases, leading to a rise of the velocity
571 (according to the Equation (1)) that promotes pollutant dispersion.

572 For the alternative scenarios in which the source diameter and the amount of fuel burnt have both
573 been modified (Q2A1 and Q5A1), the variabilities (%) generated by the SPRAY - fire model are
574 significantly higher than those obtained with the other source types (Figure 3). Indeed, when using
575 the fire model, since the diameter is almost irrelevant, the variation in the Tracer concentration is due
576 only to the increase in the amount of fuel burnt.

577 Therefore, from this first evaluation, the most relevant parameters appear to be the source diameter
578 and the amount of fuel burnt, although the latter is a parameter that can be usually quantified with a
579 certain degree of reliability.

580 **3.3 Alternative scenarios for model-specific parameters**

581 **3.3.1 CALPUFF: the influence of σ_{z0}**

582 For the CALPUFF model, the investigated parameter is the initial vertical dispersion coefficient. In
583 the $\sigma_{z0,1}$ scenario this variable has been halved compared to the base-case. The variability (%) of the
584 maximum Tracer concentration values resulting at the selected receptors from the simulation relevant
585 to the $\sigma_{z0,1}$ scenario compared to the base-case is graphically shown in the Supplementary Material
586 S4 and briefly discussed in this section of the paper.

587 From the alternative scenario, it turns out that the initial vertical dispersion coefficient does not
588 significantly affect the ground level concentrations: when passing from a σ_{z0} of 6.98 m to a σ_{z0} of
589 3.49, the model results (i.e. the concentrations at the considered receptors) are subjected to a
590 maximum variation of 9.5% corresponding to the point of maximum concentration, whereas for the
591 other receptors this variability is below 2%.

592 3.3.2 SPRAY: the influence of model-specific parameters

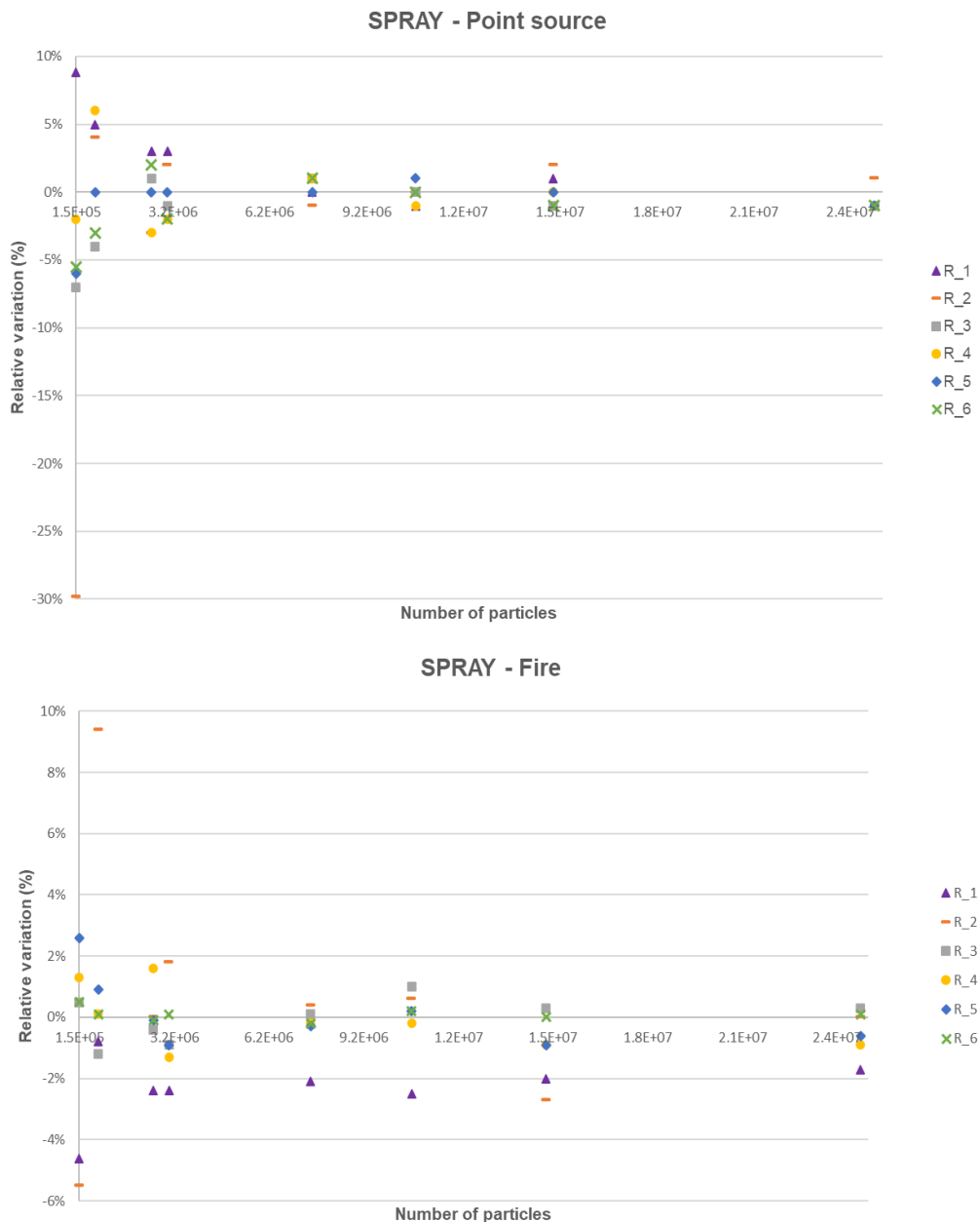
593 As mentioned in section 2.8, since SPRAY is a more advanced software, which requires the definition
594 of several parameters, different scenarios have been developed to investigate the effect of those
595 variables whose estimation is not trivial.

596 The variability (%) of the maximum Tracer concentration values at the selected receptors (1-6)
597 resulting from the alternative scenarios relevant to the SPRAY specific parameters (except for the
598 number of particles number, which will be discussed later) compared to the *base-case* has been
599 investigated. In the Supplementary Material S4, a figure showing the % variability obtained at discrete
600 receptors for the alternative scenarios is reported.

601 A first consideration concerns the percent variations resulting from the modifications of the model-
602 specific parameters compared to those of the source term parameters. None of the variations of the
603 model-specific parameters leads to significant alteration of the model outputs, as it is the case for the
604 variations applied to the source diameter or the amount of fuel.

605 Indeed, both the SPRAY – point source model and the SPRAY - fire model show, in correspondence
606 of almost all the receptors considered and for almost all the investigated parameters, a variability
607 lower than 10%. In addition, comparing the two source types, their response to the input variation is
608 very similar. The most different behaviour is the one observed for the change of the vertical dimension
609 of the “emission parallelepiped”: for the scenarios Δz_2 , Δz_3 and Δz_4 , the SPRAY - point source
610 model always shows a percent variation higher than the fire model. Thus, this behaviour does not
611 seem to be attributable to the position of the selected receptors but it is a general feature resulting
612 from the different way to model the source. Indeed, a change in Δz , which represents the vertical
613 dimension of a “box” centred in the emission region centre of gravity in which the particles initially
614 appear (see Section 2.7.2.2), means a change in the dimension of the region from which the particles
615 start to rise up due to the buoyancy. Thus, the plume rise is affected by this variable in the sense that

616 the “idealized” plume containing the particles has a different initial shape and dimension according
 617 to this parameter. On the other hand, the fire model considers a portion of emitted particles with no
 618 buoyancy flux: the rapid downfall of these particles makes this kind of simulated source less
 619 dependent on the variable Δz .



620 **Figure 4.** % variation of the maximum Tracer concentration values at the selected receptors resulting from
 621 the simulations of the alternative cases for the particles number (for SPRAY – point and SPRAY – fire)
 622 compared to the reference base-case
 623

624 Another investigated parameter is the number of particles, which determines the variabilities (%)
 625 reported in Figure 4. It is worth recalling that, when analysing the output variations due to the particles

626 number, the variabilities are not referred to the *base-case*, but to a different reference simulation
627 involving the highest amount of particles considered (i.e. 74'682'000 particles emitted in 3 hours).
628 The higher the number of particles, the lower the stochastic variability of the results.
629 As expected, for both source types, an insufficient number of particles leads to discrepancies in the
630 results, whereas the percent variation produced by the number of particles tends to decrease when the
631 input parameter becomes closer to the maximum number of particles considered. In particular, for
632 scenario PARTIC8, involving the emission of 24'896'160 particles, the percent variability is
633 approximately 1% in all the selected receptors. Considering scenario PARTIC4, which implies the
634 release of 2'989'440 particles, a maximum variability of 3% has been found. Considering the purpose
635 of the first part of this paper, which aims to investigate the model response to “macroscopic
636 variations” in the input data, a “distorted” result of 3% is considered acceptable.

637 **3.4 Sensitivity analysis**

638 The development of alternative scenarios enables to identify the most influential variables. Looking
639 at the relative variations (%) analysed for each scenario in the previous paragraphs, the most critical
640 input datum turns out to be the source diameter (except for the SPRAY - fire model). Although the
641 amount of fuel burnt also significantly affects the ground level concentrations, in the case of real fires,
642 this is usually a parameter that can be quantified with a certain degree of reliability. That is why the
643 sensitivity analysis, described in Section 2.8, has been applied only to the source diameter.

644 More in detail, the analysis has been applied to the point source simulated by SPRAY and the buoyant
645 area source of CALPUFF, where it produces the main effects (see Section 3.2).

646 As already mentioned in Section 2.8.2, the source diameter has been perturbed by 1%, 2% and 3% in
647 both directions with respect to the reference value of the *base-case*, while all the other parameters
648 were kept unchanged.

649 Thus, 12 additional simulations, 6 for CALPUFF and 6 for SPRAY, have been run, setting the source
650 diameter as reported in Table 6.

651

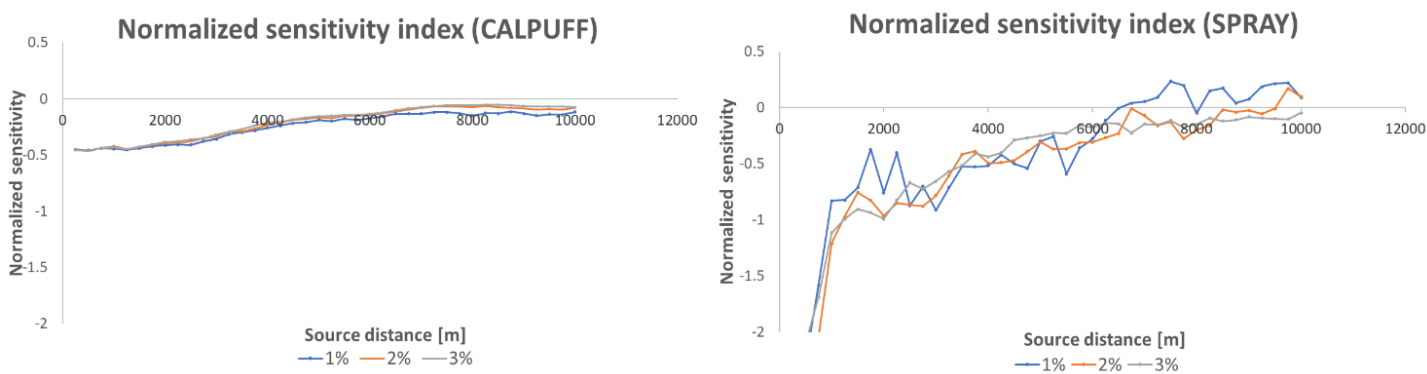
Table 6. Source diameter resulting from a variation of 1%, 2%, 3% of the average value

Average value (base-case) = 5 m					
-1%	+1%	-2%	+2%	-3%	+3%
4.95 m	5.05 m	4.90 m	5.10 m	4.85 m	5.15 m

652

653 These additional runs allowed for comparison of the sensitivity of the SPRAY model (with
654 106'688'880 particles) and the CALPUFF model related to variations of the source diameter.

655 Looking at the trend of the normalized sensitivity index on the plume axis (Figure 5), a first comment
656 concerns the sign of the coefficient. For CALPUFF, regardless of the considered receptor, the
657 sensitivity coefficient obtained by the puff model is always negative, revealing that a negative
658 correlation between the input and the output exists. The negative sign of the coefficient provides a
659 clear indication that the concentration value will be reduced because of an increment of the diameter.
660 The same general behaviour is detected in SPRAY, except for few points, where a slightly positive
661 value is obtained.



662

663 **Figure 5.** Normalized sensitivity index as a function of the source distance resulting from SPRAY (106'688'880
664 particles) and CALPUFF simulations by changing the source diameter by 1%, 2% and 3%

665 Another consideration concerns the general trend of the sensitivity coefficient as a function of the
666 source distance. Both models produce the highest values (considering the absolute value) close to the
667 source, whereas values close to zero are identified for higher distances from the source. This means
668 that the investigated parameter has a greater influence on the receptors close to the emission source.

669 This can be ascribed to the plume rise mechanism, which is largely affected by the source diameter:
670 as previously discussed (Section 3.2), a change in the buoyancy flux affects the pollutant dispersion
671 close to the emission source more than from far distances.

672 In addition, considering the receptors close to the source, higher sensitivity coefficients are obtained
673 when considering the point source simulated by SPRAY than for the CALPUFF model. As discussed
674 in Section 3.1, the simulations with the CALPUFF - buoyant area source model lead to a lower
675 buoyancy flux compared to the point source because of the heat losses. This in turn means that the
676 plume rise phenomenon is reduced, explaining why a variation in the source diameter has less
677 influence on the pollutant dispersion.

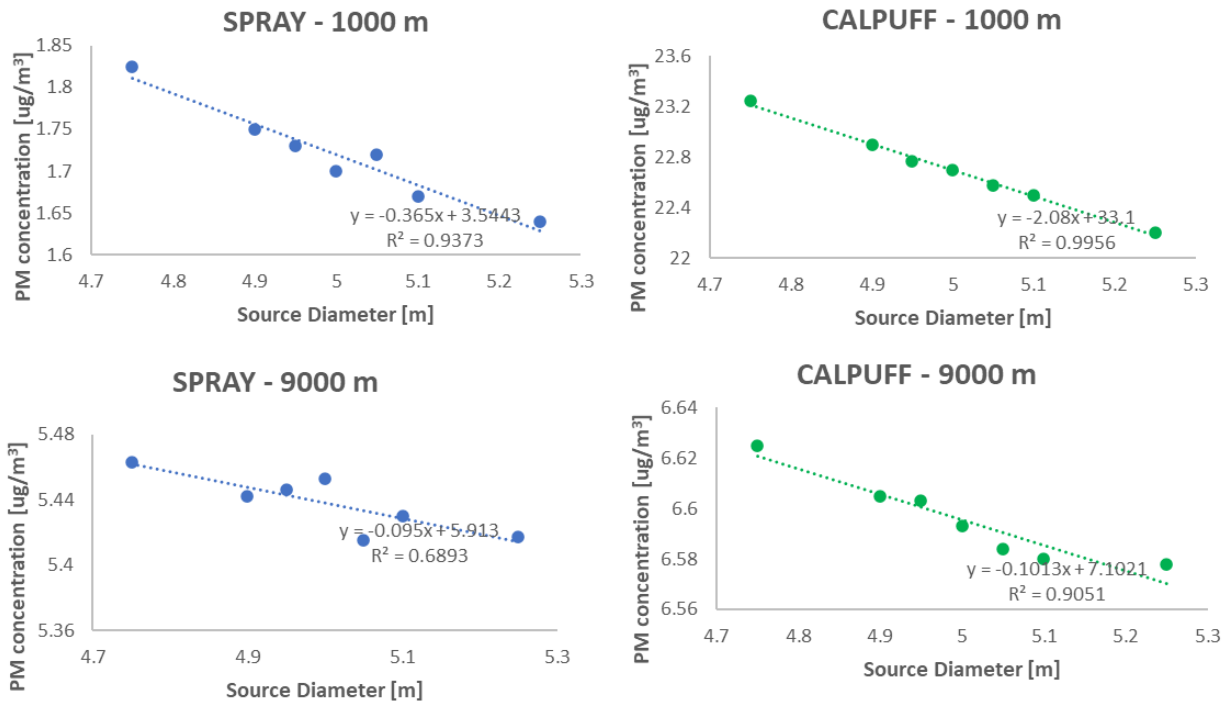
678 The obtained sensitivity indexes make it possible to identify whether there is a linear relationship
679 between the input and the output datum. As reported by Yegnan et al., 2002 , if the sensitivity
680 coefficient is constant over a range of input parameters (i.e. if there is not a change in the sensitivity
681 with a change in the input variable), the input datum can be considered to be linear with respect to
682 the output.

683 Concerning CALPUFF, as shown in Figure 5, the 3 lines are so close together that they almost
684 overlap, indicating an almost linear dependence of the ground level concentrations on the source
685 diameter. Also, the distance between the curves increases moving away from the source, and this
686 means that this linear dependence is gradually reduced.

687 On the other hand, in SPRAY simulations (run with 106'688'880 particles), the lines seem to be more
688 distant from each other. However, the scattered behaviour does not allow to clearly identify the
689 distances between the lines and, therefore, any comment concerning the input-output relationship
690 would be difficult.

691 Thus, to properly identify the relationship between the source diameter and the pollutant
692 concentration predicted by the two models, some receptors, located at different distances from the
693 source, have been considered.

694 Considering, for instance, receptors placed at a distance of 1000 m and 9000 m, respectively, from
 695 the source, the concentration trends predicted by SPRAY and CALPUFF when changing the source
 696 diameter are shown in Figure 6:



697 **Figure 6.** Maximum 1-hour Tracer concentration as a function of the source diameter predicted by the CALPUFF
 698 model (left) and by the SPRAY model (right) on two receptors located at 1000 m and 9000 m from the source,
 699 respectively
 700

701 In addition, in each plot, the trend line (linear type) is drawn, and the resulting linear expression and
 702 the correlation coefficient (R^2) are displayed.

703 Considering the receptor located at 1000 m from the source, it can be stated that the linear model
 704 properly approximates the input-output relationship. This is true for both models, even if a higher R^2
 705 value is found for CALPUFF.

706 By increasing the receptor distance from the source up to 9000 m, the R^2 coefficient decreases
 707 progressively for both models, even though a better fit is still observed for the CALPUFF model.

708 These considerations are also confirmed by the analysis of other receptors, located at different
 709 intermediate distances from the source (see Supplementary Material S5 for receptors located at 3000
 710 m, 5000 m and 7000 m from the source).

711 The analysis on the individual receptors shows a decreasing reliability of the linear relationship
712 between output and input values when moving away from the source. This may be justified
713 considering the wind effect on the dispersion phenomenon. Indeed, the Tracer concentrations
714 modelled far from the source refer to the dispersion of the pollutant that has been subjected to the
715 wind field for longer distances. The turbulent stochastic behaviour associated to the wind field
716 promotes the plume distortion, which will be more pronounced far from the emission source. This
717 observation is also confirmed, for instance, by the ground level concentration maps resulting from
718 the CALPUFF simulations when changing the source diameter from 5 m (base-case) to 10 m. The
719 maps, reported in the Supplementary Material S6, show that, in the vicinity of the source, the plume
720 direction remains practically unchanged, whereas at large distances, the wind effect results in a major
721 plume deviation.

722

723 Comparing the two models, it can be observed that, regardless of the considered receptor, the R^2
724 coefficients associated to the results of the SPRAY model are always lower than those of the
725 CALPUFF model. The stochastic behaviour of the Lagrangian model influences the trajectory of each
726 particle: the component related to the turbulent fluctuation provides to each particle a random
727 character. This chaotic contribution leads to a loss of linearity between the input and the output
728 variables.

729 To conclude, among all the information provided by this analysis, the most interesting is the one
730 related to the different sensitivities of SPRAY and CALPUFF to the investigated parameters. Indeed,
731 the particle model appears to have a higher numerical sensitivity with respect to the diameter of the
732 emission source. This discrepancy is particularly evident in the vicinity of the emission source, where
733 the sensitivity coefficients resulting from SPRAY simulations are higher by one order of magnitude.
734 On the other hand, at larger distances the sensitivities of the two models appear comparable.

735 4 CONCLUSIONS

736 When modelling the environmental effects of atmospheric pollution, many sources of imprecision
737 and uncertainty affect the results and should therefore be critically analysed. Depending on the model
738 considered, there are numerous potential sources of variability, such as the input data required by the
739 model.

740 This paper aimed to compare the sensitivity of the SPRAY and the CALPUFF models to input
741 parameters when simulating the pollutant dispersion from a hypothetical accidental fire, in order to
742 identify the most influential variables. In particular, the study focused on the effects of input data
743 regarding both source-term characterization and model-specific parameters.

744 To this purpose, starting from a reference “base-case” scenario, other alternative emission scenarios,
745 characterized by a “macroscopic variation” of each variable, have been defined. For each alternative
746 scenario, three different source types have been studied: with CALPUFF the fire is simulated as a
747 buoyant area source, whereas with SPRAY the source is simulated as a point source and as a fire
748 characterized by a 10% of emitted particles having no buoyancy flux.

749 The most relevant outcome resulting from the investigation of the alternative scenarios is that
750 CALPUFF and SPRAY sensitivities to “macroscopic variations” of the considered parameters are
751 generally comparable. The only significant difference is the model sensitivity to the source diameter
752 because, when using the specific option of the SPRAY model to simulate emission from fires, the
753 influence of the diameter turns out to be negligible. Instead, the buoyant area source modelled by
754 CALPUFF and the point source simulated by SPRAY are significantly affected by variations in the
755 estimation of the source diameter. Indeed, the simulations conducted at the boundaries of the
756 uncertainty range for the source diameter lead to variations of about 50-60% in the maximum Tracer
757 concentrations at sensitive receptors. On the other hand, when using SPRAY in combination with the
758 specific fire option, the source diameter variation gives a maximum variability of 10%. These
759 discrepancies can be explained considering the different relationships used to describe the plume rise

760 phenomenon in the different models (see Section 3.2). It should be highlighted that the choice of the
761 emission model that best approximates the real physical behaviour is essentially left to the user.

762 All the other investigated variables concerning the source term characteristics, such as source height
763 and emission temperature, do not significantly affect the model outputs, generally giving a maximum
764 variation in pollutant concentrations simulated at the receptors of about 10%. The model-specific
765 parameters point out a non-controlling influence on the model results, generally producing variations
766 of about 10% in the results as well.

767 Thus, in conclusion the most relevant parameters in terms of model sensitivity turned out to be the
768 source diameter and the amount of fuel burnt, although the latter can usually be quantified with a
769 certain degree of reliability. Looking at the % variations relevant to the simulations of the alternative
770 scenarios, the source height seems the third most influential parameter, even though its influence on
771 the model results is limited (about 10%). The temperature of the emission source and the investigated
772 model-specific parameters lead to almost negligible variations.

773 However, it is worth recalling that the diameter is the parameter that leads to greater variability, but
774 it is also one of those that has been varied most in the alternative scenarios. This is because the
775 estimation of the source diameter is particularly critical and, consequently, a sufficiently wide range
776 of variability had to be considered.

777 Another observation arising from the first part is related to the discrepancies obtained when using the
778 different source options. In this regard, modelling the fire as a point source is not recommended, since
779 it tends to underestimate ground concentrations. The use of the specific fire options existing both for
780 CALPUFF (buoyant area source) and SPRAY (fire option), which generally produce comparable
781 ground concentration trends as a function of the distance from the source (Figure 2), is actually
782 recommended.

783 To effectively evaluate the model sensitivity to the source diameter regardless of the reasonable range
784 of variability, the sensitivity analysis has been performed by applying a “microscopic variation” to
785 this parameter.

786 The most remarkable outcome resulting from this second approach is that the SPRAY – point source
787 model shows a significantly higher sensitivity to the source diameter (of an order of magnitude) than
788 CALPUFF near the emission source. Conversely, at larger distances, the sensitivity of the two models
789 seems comparable.

790 This work allowed to evaluate the sensitivities of the SPRAY and CALPUFF models to the
791 investigated parameters from a theoretical and numerical point of view. However, this paper is not
792 intended to present a sensitivity study applicable to any model or to any case study, but rather it points
793 out the importance of carrying out an investigation of the possible range of variation of the input data
794 in order to identify the most influential variables. The obtained results can be useful to different
795 stakeholders (model users, environmental and control agencies) to have a deeper knowledge of the
796 possible range of variation of the simulated ground concentration values deriving from the
797 uncertainties in the definition of the model input data.

798 It should be highlighted that the aim of this work is not to assess the exactness of atmospheric
799 dispersion models: to evaluate the accuracy of the modelling results, in case of real accidental fires,
800 the sensitivity analysis should be coupled with some experimental validation in order to evaluate the
801 model capability to predict the experimental observations and, possibly, to improve and optimize its
802 performances.

803

804 **Acknowledgements**

805 The authors want to thank ARIANET for supporting the implementation of the case study with the
806 SPRAY model.

807 **Funding**

808 This research did not receive any specific grant from funding agencies in the public, commercial, or
809 not-for-profit sectors.

810 **References**

- 811 Adame, J.A., Lope, L., Hidalgo, P.J., Sorribas, M., Gutiérrez-Álvarez, I., del Águila, A., Saiz-
812 Lopez, A., Yela, M., 2018. Study of the exceptional meteorological conditions, trace gases and
813 particulate matter measured during the 2017 forest fire in Doñana Natural Park, Spain. *Sci.*
814 *Total Environ.* 645, 710–720. <https://doi.org/10.1016/j.scitotenv.2018.07.181>
- 815 Ainslie, B., Jackson, P.L., 2009. The use of an atmospheric dispersion model to determine influence
816 regions in the Prince George, B.C. airshed from the burning of open wood waste piles. *J.*
817 *Environ. Manage.* 90, 2393–2401. <https://doi.org/10.1016/j.jenvman.2008.11.009>
- 818 Antonioni, G., Burkhart, S., Burman, J., Dejoan, A., Fusco, A., Gaasbeek, R., Gjesdal, T., Jäppinen,
819 A., Riikonen, K., Morra, P., Parmhed, O., Santiago, J.L., 2012. Comparison of CFD and
820 operational dispersion models in an urban-like environment. *Atmos. Environ.* 47, 365–372.
821 <https://doi.org/10.1016/j.atmosenv.2011.10.053>
- 822 ARIANET, 2011. SURFPRO3 User's guide (SURFaceatmosphere interface PROcessor, Version 3).
823 <https://www.aria-net.it/it/>.
- 824 Bhuiyan, A.A., Naser, J., 2015. Computational modelling of co-firing of biomass with coal under
825 oxy-fuel condition in a small scale furnace. *Fuel* 143, 455–466.
826 <https://doi.org/10.1016/j.fuel.2014.11.089>
- 827 Björnham, O., Grahn, H., Burman, J., 2020. Comparison of the predictive results from the two
828 dispersion models PUMA and LPELLO with the JR II field data. *Atmos. Environ.* 233.
829 <https://doi.org/10.1016/j.atmosenv.2020.117521>
- 830 Booher, L.E., Janke, B., 1997. Air emissions from petroleum hydrocarbon fires during controlled
831 burning. *Am. Ind. Hyg. Assoc. J.* 58, 359–365. <https://doi.org/10.1080/15428119791012720>
- 832 BS EN 1363-2, 1999. Fire resistance tests. Part 2: Alternative and additional procedures.

833 Cécé, R., Bernard, D., Brioude, J., Zahibo, N., 2016. Microscale anthropogenic pollution modelling
834 in a small tropical island during weak trade winds: Lagrangian particle dispersion simulations
835 using real nested LES meteorological fields. *Atmos. Environ.* 139, 98–112.
836 <https://doi.org/10.1016/j.atmosenv.2016.05.028>

837 Chang, J.I., Lin, C.C., 2006. A study of storage tank accidents. *J. Loss Prev. Process Ind.* 19, 51–59.
838 <https://doi.org/10.1016/j.jlp.2005.05.015>

839 Chettouh, S., Hamzi, R., Innal, F., Haddad, D., 2014. Industrial fire simulation and uncertainty
840 associated with the Emission Dispersion Model. *Clean Technol. Environ. Policy* 16, 1265–
841 1273. <https://doi.org/10.1007/s10098-014-0792-x>

842 Chutia, R., Mahanta, S., Datta, D., 2014. Uncertainty modelling of atmospheric dispersion by
843 stochastic response surface method under aleatory and epistemic uncertainties. *Sadhana -*
844 *Acad. Proc. Eng. Sci.* 39, 467–485. <https://doi.org/10.1007/s12046-013-0212-7>

845 Daly, A., Zannetti, P., Echekeki, T., 2012. A combination of fire and dispersion modeling techniques
846 for simulating a warehouse fire. *Int. J. Saf. Secur. Eng.* 2, 368–380.
847 <https://doi.org/10.2495/SAFE-V2-N4-368-380>

848 Devenish, B.J., Francis, P.N., Johnson, B.T., Sparks, R.S.J., Thomson, D.J., 2012. Sensitivity
849 analysis of dispersion modeling of volcanic ash from Eyjafjallajökull in May 2010. *J.*
850 *Geophys. Res. Atmos.* 117, 1–21. <https://doi.org/10.1029/2011JD016782>

851 DiNenno, P., Drysdale, D., Beyler, C., Walton, W., Custer, R., Hall, J., 2002. *SFPE handbook of*
852 *fire protection engineering*, 3rd ed. Quincy, Massachusetts.

853 Elbir, T., 2003. Comparison of model predictions with the data of an urban air quality monitoring
854 network in Izmir, Turkey. *Atmos. Environ.* 37, 2149–2157. [https://doi.org/10.1016/S1352-](https://doi.org/10.1016/S1352-2310(03)00087-6)
855 [2310\(03\)00087-6](https://doi.org/10.1016/S1352-2310(03)00087-6)

856 Elbir, T., Mangir, N., Kara, M., Simsir, S., Eren, T., Ozdemir, S., 2010. Development of a GIS-
857 based decision support system for urban air quality management in the city of Istanbul. *Atmos.*

858 Environ. 44, 441–454. <https://doi.org/10.1016/j.atmosenv.2009.11.008>

859 Gant, S.E., Kelsey, A., McNally, K., Witlox, H., Bilio, M., 2013. Sensitivity analysis of dispersion
860 models for jet releases of dense-phase carbon dioxide. *Chem. Eng. Trans.* 31, 121–126.
861 <https://doi.org/10.3303/CET1331021>

862 Gonsamo, A., 2011. Normalized sensitivity measures for leaf area index estimation using three-
863 band spectral vegetation indices. *Int. J. Remote Sens.* 32, 2069–2080.
864 <https://doi.org/10.1080/01431161.2010.502153>

865 Griffiths, S.D., Chappell, P., Entwistle, J.A., Kelly, F.J., Deary, M.E., 2018. A study of particulate
866 emissions during 23 major industrial fires: Implications for human health. *Environ. Int.* 112,
867 310–323. <https://doi.org/10.1016/j.envint.2017.12.018>

868 Hanna, S.R., Britter, R.E., 2002. Wind Flow and Vapor Cloud Dispersion at Industrial and Urban
869 Sites, Wind Flow and Vapor Cloud Dispersion at Industrial and Urban Sites.
870 <https://doi.org/10.1002/9780470935613>

871 Henderson, S.B., Burkholder, B., Jackson, P.L., Brauer, M., Ichoku, C., 2008. Use of MODIS
872 products to simplify and evaluate a forest fire plume dispersion model for PM10 exposure
873 assessment. *Atmos. Environ.* 42, 8524–8532. <https://doi.org/10.1016/j.atmosenv.2008.05.008>

874 Holmes, N.S., Morawska, L., 2006. A review of dispersion modelling and its application to the
875 dispersion of particles: An overview of different dispersion models available. *Atmos. Environ.*
876 40, 5902–5928. <https://doi.org/10.1016/j.atmosenv.2006.06.003>

877 Holnicki, P., Kałuszko, A., Trapp, W., 2016. An urban scale application and validation of the
878 CALPUFF model. *Atmos. Pollut. Res.* 7, 393–402. <https://doi.org/10.1016/j.apr.2015.10.016>

879 Holnicki, P., Nahorski, Z., 2015. Emission Data Uncertainty in Urban Air Quality Modeling—Case
880 Study. *Environ. Model. Assess.* 20, 583–597. <https://doi.org/10.1007/s10666-015-9445-7>

881 Ingason, H., Li, Y.Z., 2015. Tunnel Fire Dynamics. <https://doi.org/10.1007/978-1-4939-2199-7>

882 Invernizzi, M., Brancher, M., Sironi, S., Capelli, L., Piringer, M., Schaubberger, G., 2020. Odour

883 impact assessment by considering short-term ambient concentrations: A multi-model and two-
884 site comparison. *Environ. Int.* 144, 105990. <https://doi.org/10.1016/j.envint.2020.105990>

885 Invernizzi, M., Tagliaferri, F., Sironi, S., Tinarelli, G., Capelli, L., 2021. Simulating Pollutant
886 Dispersion from Accidental Fires with a Focus on Source Characterization. *J. Heal. Pollut.* 11.
887 <https://doi.org/10.5696/2156-9614-11.30.210612>

888 Islam, M.A., 1999. Application of a Gaussian Plume model to determine the location of an
889 unknown emission source. *Water. Air. Soil Pollut.* 112, 241–245.
890 <https://doi.org/10.1023/A:1005047321015>

891 Jang, C.B., Choi, S.W., Baek, J.B., 2015. CFD modeling and fire damage analysis of jet fire on
892 hydrogen pipeline in a pipe rack structure. *Int. J. Hydrogen Energy* 40, 15760–15772.
893 <https://doi.org/10.1016/j.ijhydene.2015.09.070>

894 Jung, Y.R., Park, W.G., Park, O.H., 2003. Pollution dispersion analysis using the puff model with
895 numerical flow field data. *Mech. Res. Commun.* 30, 277–286. [https://doi.org/10.1016/S0093-6413\(03\)00024-7](https://doi.org/10.1016/S0093-6413(03)00024-7)

896

897 Kota, S.H., Ying, Q., Zhang, Y., 2013. Simulating near-road reactive dispersion of gaseous air
898 pollutants using a three-dimensional Eulerian model. *Sci. Total Environ.* 454–455, 348–357.
899 <https://doi.org/10.1016/j.scitotenv.2013.03.039>

900 Langmann, B., Duncan, B., Textor, C., Trentmann, J., van der Werf, G.R., 2009. Vegetation fire
901 emissions and their impact on air pollution and climate. *Atmos. Environ.* 43, 107–116.
902 <https://doi.org/10.1016/j.atmosenv.2008.09.047>

903 Leelőssy, Á., Molnár, F., Izsák, F., Havasi, Á., Lagzi, I., Mészáros, R., 2014. Dispersion modeling
904 of air pollutants in the atmosphere: a review. *Cent. Eur. J. Geosci.* 6, 257–278.
905 <https://doi.org/10.2478/s13533-012-0188-6>

906 Lemieux, P.M., Lutes, C.C., Santoianni, D.A., 2004. Emissions of organic air toxics from open
907 burning: A comprehensive review, *Progress in Energy and Combustion Science.*

908 <https://doi.org/10.1016/j.pecs.2003.08.001>

909 Liu, T., Marlier, M.E., DeFries, R.S., Westervelt, D.M., Xia, K.R., Fiore, A.M., Mickley, L.J.,
910 Cusworth, D.H., Milly, G., 2018. Seasonal impact of regional outdoor biomass burning on air
911 pollution in three Indian cities: Delhi, Bengaluru, and Pune. *Atmos. Environ.* 172, 83–92.
912 <https://doi.org/10.1016/j.atmosenv.2017.10.024>

913 Liu, X., Godbole, A., Lu, C., Michal, G., Venton, P., 2015. Optimisation of dispersion parameters
914 of Gaussian plume model for CO₂ dispersion. *Environ. Sci. Pollut. Res.* 22, 18288–18299.
915 <https://doi.org/10.1007/s11356-015-5404-8>

916 Markatos, N.C., Christolis, C., Argyropoulos, C., 2009. Mathematical modeling of toxic pollutants
917 dispersion from large tank fires and assessment of acute effects for fire fighters. *Int. J. Heat
918 Mass Transf.* 52, 4021–4030. <https://doi.org/10.1016/j.ijheatmasstransfer.2009.03.039>

919 Mishra, K.B., Wehrstedt, K.D., 2015. Underground gas pipeline explosion and fire: CFD based
920 assessment of foreseeability. *J. Nat. Gas Sci. Eng.* 24, 526–542.
921 <https://doi.org/10.1016/j.jngse.2015.04.010>

922 Nivolianitou, Z., Konstandinidou, M., Michalis, C., 2006. Statistical analysis of major accidents in
923 petrochemical industry notified to the major accident reporting system (MARS). *J. Hazard.
924 Mater.* 137, 1–7. <https://doi.org/10.1016/j.jhazmat.2004.12.042>

925 Novozhilov, V., 2001. Computational fluid dynamics modeling of compartment fires. *Prog. Energy
926 Combust. Sci.* 27, 611–666. [https://doi.org/10.1016/S0360-1285\(01\)00005-3](https://doi.org/10.1016/S0360-1285(01)00005-3)

927 Ravina, M., Panepinto, D., Zanetti, M.C., 2020. Development of the DIDEM Model: Comparative
928 evaluation of CALPUFF and SPRAY dispersion models. *Int. J. Environ. Impacts Manag.
929 Mitig. Recover.* 3, 1–18. <https://doi.org/10.2495/ei-v3-n1-1-18>

930 Rodrigues, H.S., Monteiro, M.T.T., Torres, D.F.M., 2013. Sensitivity Analysis in a Dengue
931 Epidemiological Model. *Conf. Pap. Math.* 2013, 1–7. <https://doi.org/10.1155/2013/721406>

932 Russell, A., Dennis, R., 2000. NARSTO critical review of photochemical models and modeling.

933 Atmos. Environ. 34, 2283–2324. [https://doi.org/10.1016/S1352-2310\(99\)00468-9](https://doi.org/10.1016/S1352-2310(99)00468-9)

934 Rzeszutek, M., 2019. Parameterization and evaluation of the CALMET/CALPUFF model system in
935 near-field and complex terrain - Terrain data, grid resolution and terrain adjustment method.
936 Sci. Total Environ. 689, 31–46. <https://doi.org/10.1016/j.scitotenv.2019.06.379>

937 Santiago, J.L., Martín, F., 2008. SLP-2D: A new Lagrangian particle model to simulate pollutant
938 dispersion in street canyons. Atmos. Environ. 42, 3927–3936.
939 <https://doi.org/10.1016/j.atmosenv.2007.05.038>

940 Scire, J.S., Strimaitis, D.G., Yamartino, R.J., 2000. A User’s Guide for the CALPUFF Dispersion
941 Model. Earth Tech. Inc 521.

942 Seibert, P., 2000. Uncertainties in Atmospheric Dispersion Modelling and Source Determination.
943 Proceedings Informal Work. Meteorol. Model. Support CTBT, Vienna 1–4.

944 Seland, Oø., Iversen, T., 1999. A scheme for black carbon and sulphate aerosols tested in a
945 hemispheric scale, Eulerian dispersion model. Atmos. Environ. 33, 2853–2879.
946 [https://doi.org/10.1016/S1352-2310\(98\)00389-6](https://doi.org/10.1016/S1352-2310(98)00389-6)

947 Shie, R.H., Chan, C.C., 2013. Tracking hazardous air pollutants from a refinery fire by applying on-
948 line and off-line air monitoring and back trajectory modeling. J. Hazard. Mater. 261, 72–82.
949 <https://doi.org/10.1016/j.jhazmat.2013.07.017>

950 Sinha, N., Ghose, M.K., Singh, G., Srivastava, S., Sinha, I.N., 2004. Classification of Air Pollution
951 Dispersion Models : a Critical Review. Proc. Natl. Semin. Environ. Eng. with Spec. Emphas.
952 Min. Environ. 2004–19.

953 Sonnemans, P.J.M., Körvers, P.M.W., Pasman, H.J., 2010. Accidents in “normal” operation - Can
954 you see them coming? J. Loss Prev. Process Ind. 23, 351–366.
955 <https://doi.org/10.1016/j.jlp.2010.01.001>

956 Souto, M.J., Souto, J.A., Pérez-Muñuzuri, V., Casares, J.J., Bermúdez, J.L., 2001. A comparison of
957 operational Lagrangian particle and adaptive puff models for plume dispersion forecasting.

958 Atmos. Environ. 35, 2349–2360. [https://doi.org/10.1016/S1352-2310\(00\)00537-9](https://doi.org/10.1016/S1352-2310(00)00537-9)

959 Srinivas, C. V., Hari Prasad, K.B.R.R., Naidu, C. V., Baskaran, R., Venkatraman, B., 2016.

960 Sensitivity Analysis of Atmospheric Dispersion Simulations by FLEXPART to the WRF-

961 Simulated Meteorological Predictions in a Coastal Environment. Pure Appl. Geophys. 173,

962 675–700. <https://doi.org/10.1007/s00024-015-1104-z>

963 Tinarelli, G., 2017. SPRAY 3 . 1 - General Description and User ' s guide.

964 UNI 10796, 2009. Valutazione della dispersione in atmosfera di effluenti aeriformi.

965 <http://store.uni.com/catalogo/uni-10796-2000>.

966 UNI 10964, 2009. Guida alla selezione dei modelli matematici per la previsione di impatto sulla

967 qualità dell ' aria evaluation of air quality impact. [http://store.uni.com/catalogo/uni-10964-](http://store.uni.com/catalogo/uni-10964-2001?josso_back_to=http://store.uni.com/josso-security-check.php&josso_cmd=login_o)

968 [2001?josso_back_to=http://store.uni.com/josso-security-check.php&josso_cmd=login_o](http://store.uni.com/josso-security-check.php&josso_cmd=login_o).

969 US EPA, 1998. AP-42, “Compilation of Air Emission Factors” Chapter 1: External Combustion

970 Sources. <https://www.epa.gov/nscep>.

971 US EPA, 1995. B-95, User's guide for the industrial source complex (ISC3) dispersion models -

972 volume ii - description of model algorithms. <https://www.epa.gov/nscep>, 5th ed.

973 Weichenthal, S., Van Rijswijk, D., Kulka, R., You, H., Van Ryswyk, K., Willey, J., Dugandzic, R.,

974 Sutcliffe, R., Moulton, J., Baike, M., White, L., Charland, J.P., Jessiman, B., 2015. The impact

975 of a landfill fire on ambient air quality in the north: A case study in Iqaluit, Canada. Environ.

976 Res. 142, 46–50. <https://doi.org/10.1016/j.envres.2015.06.018>

977 Yegnan, A., Williamson, D.G., Graettinger, A.J., 2002. Uncertainty analysis in air dispersion

978 modeling. Environ. Model. Softw. 17, 639–649. [https://doi.org/10.1016/S1364-](https://doi.org/10.1016/S1364-8152(02)00026-9)

979 [8152\(02\)00026-9](https://doi.org/10.1016/S1364-8152(02)00026-9)

980 Zheng, B., Chen, G., 2011. Storage Tank Fire Accidents. Process Saf. Prog. 30, 291–293.

SUPPLEMENTARY MATERIAL S1: A SENSITIVITY ANALYSIS APPLIED TO SPRAY AND CALPUFF MODELS WHEN SIMULATING DISPERSION FROM INDUSTRIAL FIRES

Francesca Tagliaferri, Marzio Invernizzi, Laura Capelli

Δz : sketch of the emission parallelepiped required as input data by the SPRAY model

shows the emission parallelepiped (“the purple box”), highlighting its vertical dimension Δz , and its position with respect to the emission source (the white parallelepiped). In the picture below (**Errore. L'origine riferimento non è stata trovata.**), as in the considered case study, the Z_0 coordinate has been assumed coincident with the source height.

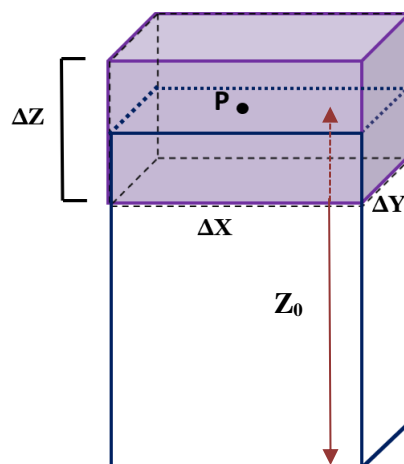


Figure 7. Emission parallelepiped and its position with respect to the emission source.

SUPPLEMENTARY MATERIAL S2: A SENSITIVITY ANALYSIS APPLIED TO SPRAY AND CALPUFF MODELS WHEN SIMULATING DISPERSION FROM INDUSTRIAL FIRES

Francesca Tagliaferri, Marzio Invernizzi, Laura Capelli

Feasibility study on the sensitivity analysis to the SPRAY model

Before starting the sensitivity analysis, it is necessary to verify its applicability to the SPRAY model: from the alternative scenarios for model specific parameters, the influence of the particles number clearly emerges. For the particles number, the “best value” would correspond, ideally, to an infinite number of emitted particles and, in practice, to a very high particles number.

Therefore, aiming the applied sensitivity analysis to identify the influence of the only selected parameter (i.e. source diameter), it is necessary to ensure that the output variability is only attributable to the variation in the source diameter

and not also to the choice of the selected number of particles. In other words, it should be verified that the particles number, does not affect the difference between concentration values (and so, the sensitivity index) resulting from simulations with same number of particles but different diameters.

For this reason, it has been decided to compare the results obtained from the SPRAY sensitivity analysis with two different numbers of particles: 2'989'400 particles, which is the value adopted in the *base-case*, and 106'688'880 particles, which may be considered as the most representative value. If the resulting sensitivity coefficients are nearly equal, the stochastic contribution of the particles number can be considered negligible and output variation can be attributed solely to the source diameter.

First, the 1% variation in the source diameter has been considered: Figure 8 shows two plots, obtained for different numbers of particles (2'989'400 and 106'688'880 emitted particles), representing the concentration trends as a function of the distance from the source. In each plot 3 curves, resulting from simulations with different values of source diameter (in particular, the diameter has been varied by $\pm 1\%$ compared to the reference value), are shown.

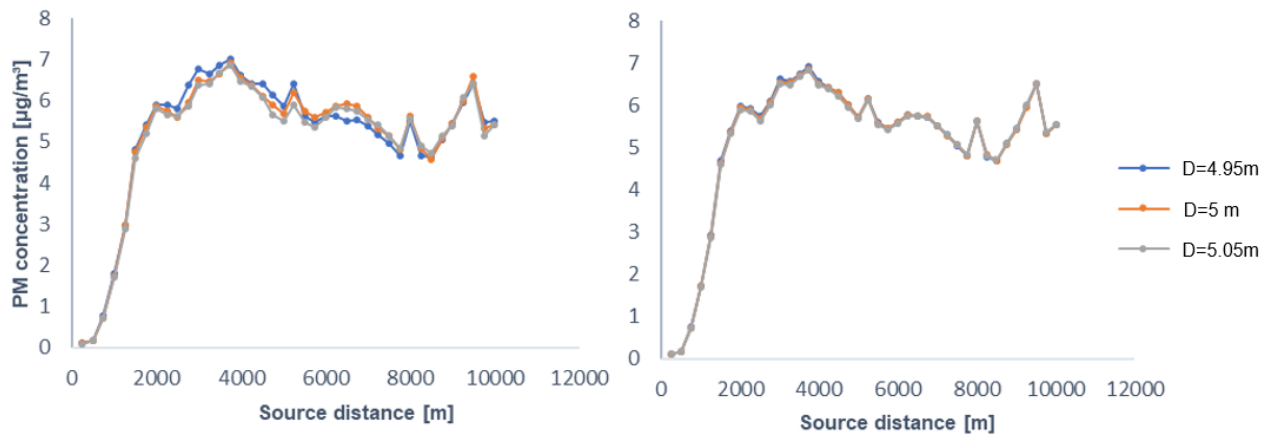


Figure 8. Maximum 1-hour PM concentration as a function of the source distance resulting from simulations with 2'989'400 particles (left) and 106'688'880 particles (right) by changing the source diameter of 1%

This figure shows that the particles number affects the sensitivity analysis: when considering 106'688'880 particles the 3 curves are very close to each other, in the other case they are clearly distinguishable from each other. Thus, for a 1% of variation in the source diameter, the output variations are also affected by the number of particles. This is confirmed by the normalized sensitivity index, whose value is dependent on the number of particles selected for the simulations, as shown in Figure 9 **Errore. L'origine riferimento non è stata trovata.** When using 2'989'400 particles, a very scattered curve is obtained. Here, it is difficult to identify a precise trend of the sensitivity index with the distance from the source. On the other hand, increasing the particles number, an approximately monotonic trend can be observed. This behaviour can be explained in view of the different impact of “model background noise” caused by the choice of the particles number. As explained in section 2.6.4, lower numbers of particles lead to results less reliable and precise, thus in the simulation with

2'989'400 particles, the stochastic contribution is more noticeable resulting in a “more disordered trend”.

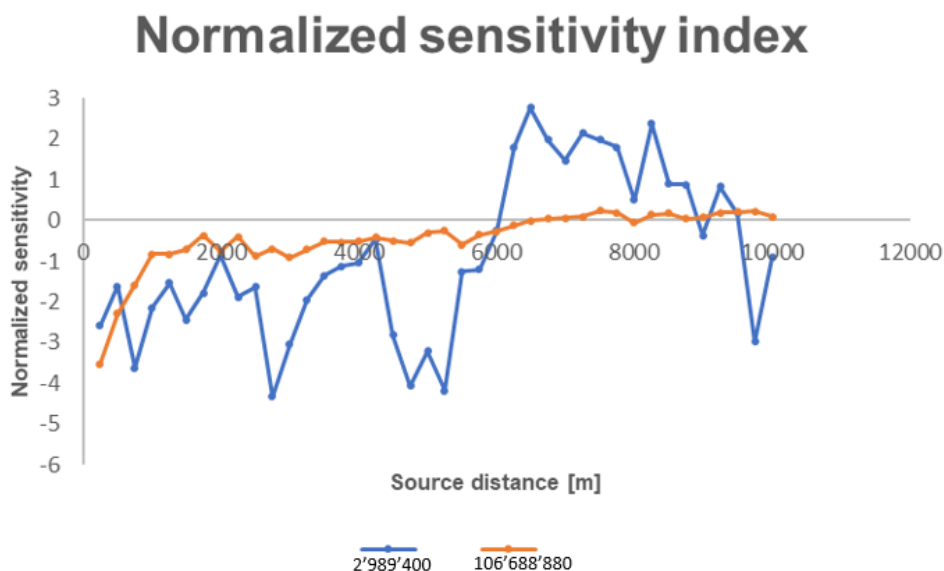


Figure 9. Normalized sensitivity index as a function of the source distance resulting from simulations with 2'989'400 particles and 106'688'880 particles by changing the source diameter of 1%

Then, the input variability has been increased up to 2% and the same plots have been developed. In particular, the concentration trends with the source distance (Figure 10) obtained with 2'989'400 and 106'688'880 particles look more like each other than those obtained by changing the source diameter of 1%. The same happens to the normalized sensitivity index (Figure 11 **Errore. L'origine riferimento non è stata trovata.**). As expected, by increasing the % variation of the input parameter, the influence of the particles number on the sensitivity analysis is progressively hidden since the concentration variation provided by the change in the diameter is of higher order of magnitude of those produced by the number of particles.

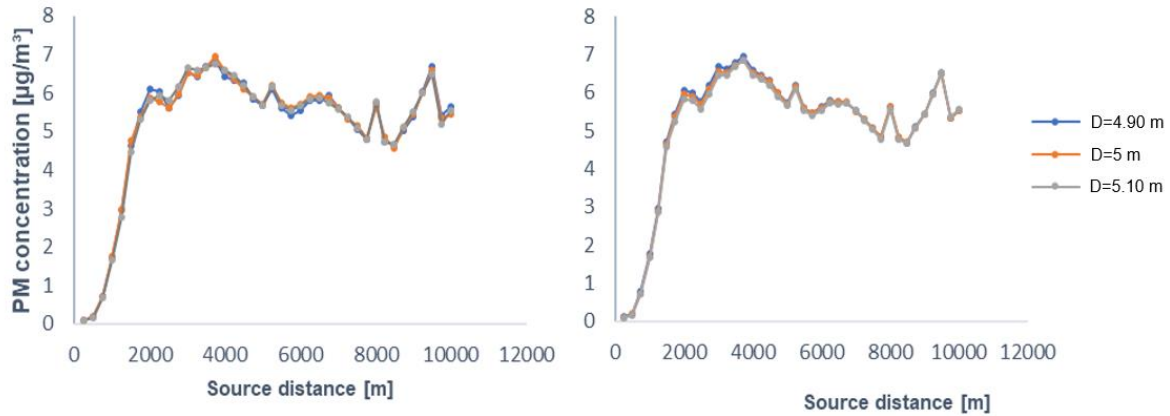


Figure 10. Maximum 1-hour PM concentration as a function of the source distance resulting from simulations with 2'989'400 particles (left) and 106'688'880 particles (right) by changing the source diameter of 2%

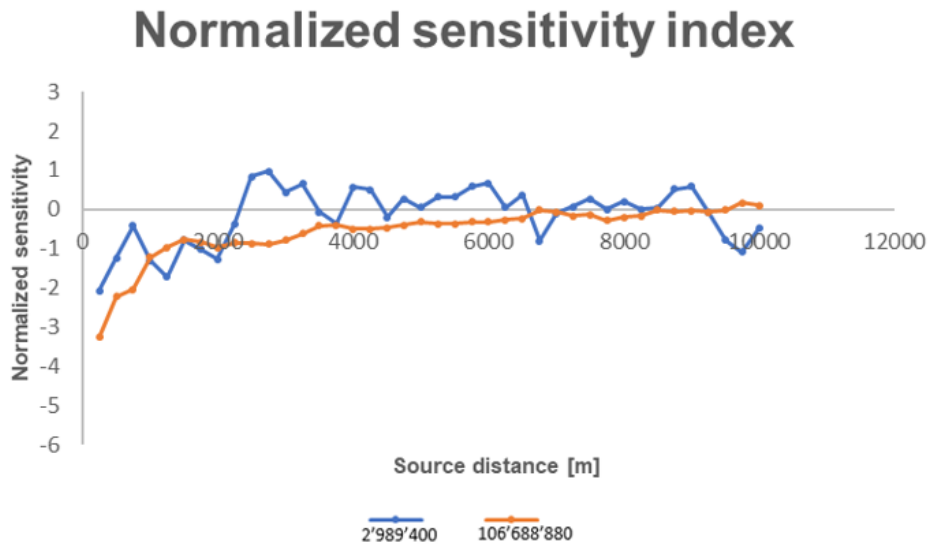


Figure 11. Normalized sensitivity index as a function of the source distance resulting from simulations with 2'989'400 particles and 106'688'880 particles by changing the source diameter of 2%

Finally, the diameter has been modified considering a variation of 3% with respect to the “nominal value” (the one of the *base-case*). The differences between the concentration trends (Figure 12) obtained at different particles numbers are less marked than those observed assuming a small change in the source diameter.

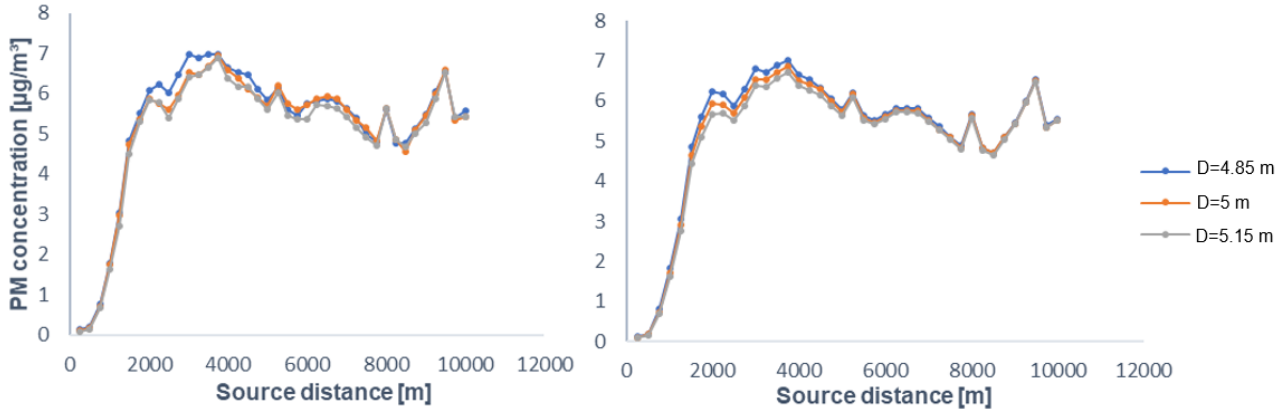


Figure 12. Maximum 1-hour PM concentration as a function of the source distance resulting from simulations with 2'989'400 particles (left) and 106'688'880 particles (right) by changing the source diameter of 3%

The same happens for the normalized sensitivity index (Figure 13). Except for receptors very close to the source, the index is mostly between -1 and 0 regardless of the number of particles. Also, differently from the previous simulations, the sensitivity indexes obtained with 2'989'400 and 106'688'880 particles show the same trend on the plume axis: the highest values are detected close to the source, at greater distances the indexes are significantly lower and very similar regardless of the source distance and the particles number.

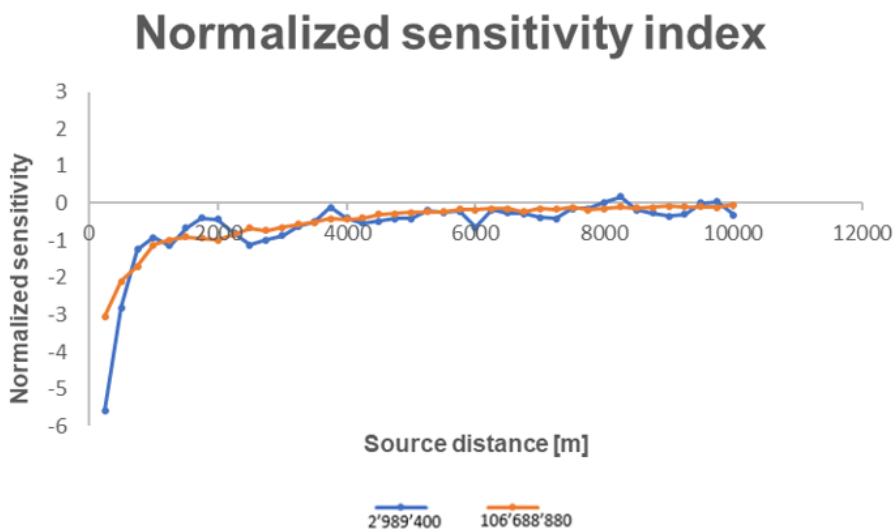


Figure 13. Normalized sensitivity index as a function of the source distance resulting from simulations with 2'989'400 particles and 106'688'880 particles by changing the source diameter of 3%

This preliminary analysis highlights the unsuitability of the approach proposed by Yegnan et al. when imposing too low variations of the input parameter and adopting 2'989'400 emitted particles. If the change imposed for the input parameter is too small, the variability in the result may be of the same order of magnitude as the one produced by the stochastic behaviour associated to the considered particles number. On the other hand, when a stronger variability is imposed to the input datum, the expected output variation is higher. Therefore, the sensitivity indexes obtained with different particles numbers are very similar.

It follows that, considering a particles number of 2'989'400, the only meaningful sensitivity analysis is the one developed with a 3% of variation of the source diameter, since the other results are altered by the selected number of particles.

SUPPLEMENTARY MATERIAL S3: A SENSITIVITY ANALYSIS APPLIED TO SPRAY AND CALPUFF MODELS WHEN SIMULATING DISPERSION FROM INDUSTRIAL FIRES

Francesca Tagliaferri, Marzio Invernizzi, Laura Capelli

WIND FIELD COMPUTED BY SWIFT vs. CALMET

Wind Field elaborated by the meteorological processor SWIFT (Figure 14) and CALMET (Figure 15) for the same hour of simulation.

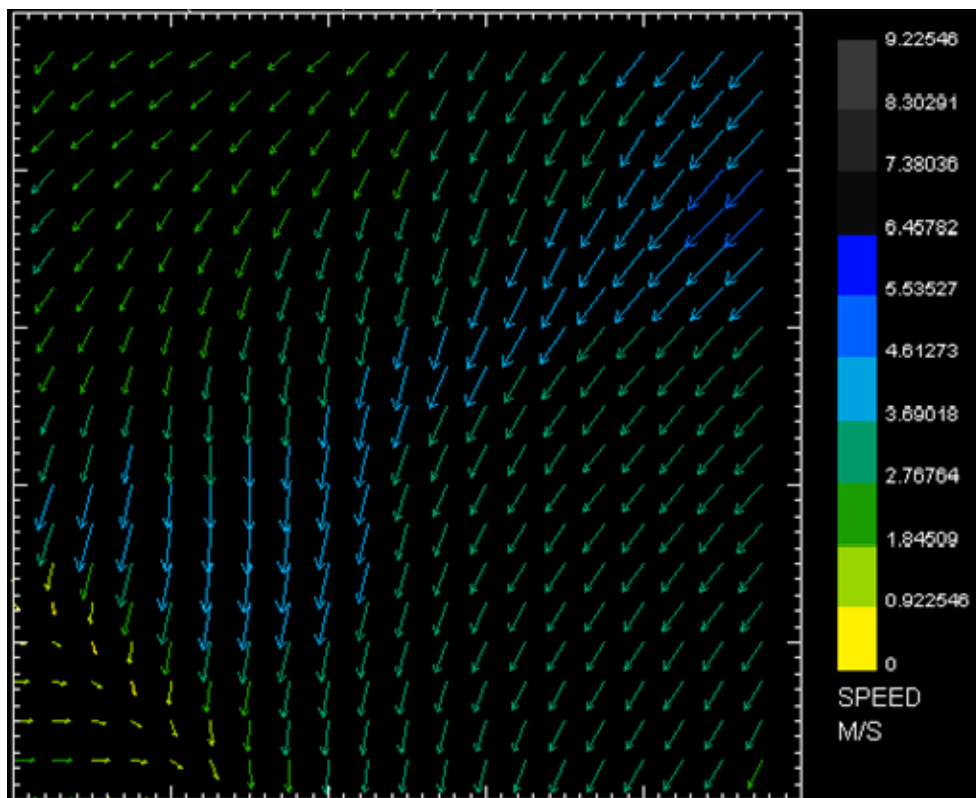


Figure 14. Wind field at 10 m elaborated by SWIFT

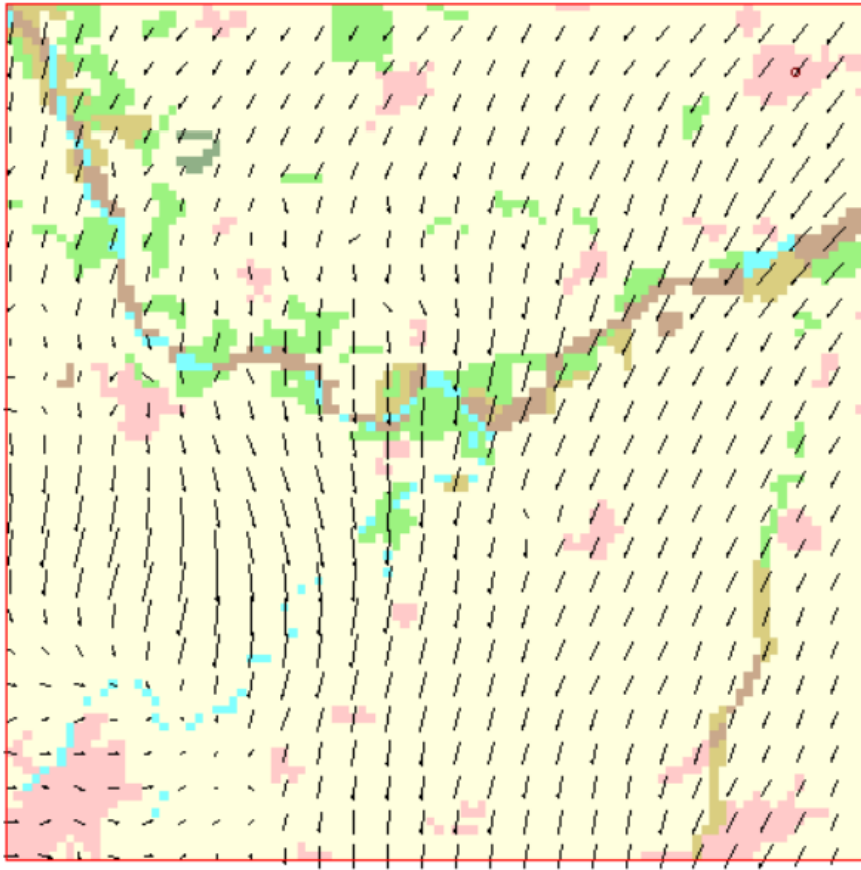


Figure 15. Wind field at 10 m elaborated by CALMET

SUPPLEMENTARY MATERIAL S4: A SENSITIVITY ANALYSIS APPLIED TO SPRAY AND CALPUFF MODELS WHEN SIMULATING DISPERSION FROM INDUSTRIAL FIRES

Francesca Tagliaferri, Marzio Invernizzi, Laura Capelli

Alternative scenarios for source geometrical features and emission scenario characteristics

CALPUFF: the influence of σ_{z0}

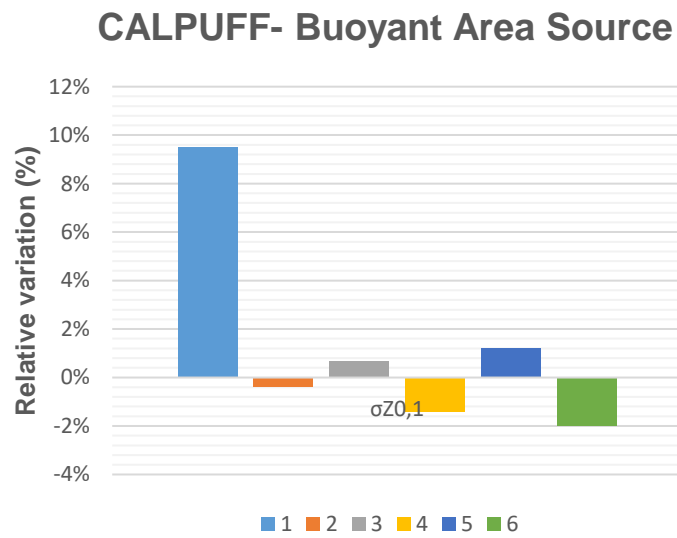


Figure 16. % variation of the maximum PM concentration values at the selected receptors resulting from the simulation of the $\sigma_{z0,1}$ emission scenario compared to the reference base-case

SPRAY: the influence of model specific parameters



Figure 17. % variation of the maximum PM concentration values at the selected receptors resulting from the simulations of the alternative cases for model specific parameters of SPRAY – point source (left) and SPRAY – fire (right) compared to the reference base-case

SUPPLEMENTARY MATERIAL S5: A SENSITIVITY ANALYSIS APPLIED TO SPRAY AND CALPUFF MODELS WHEN SIMULATING DISPERSION FROM INDUSTRIAL FIRES

Francesca Tagliaferri, Marzio Invernizzi, Laura Capelli

Relationship between the source diameter and the Tracer concentration at different distances from the source

Concentrations predicted by CALPUFF and SPRAY, on a receptor located at 3000 m from the source, at different source areas.

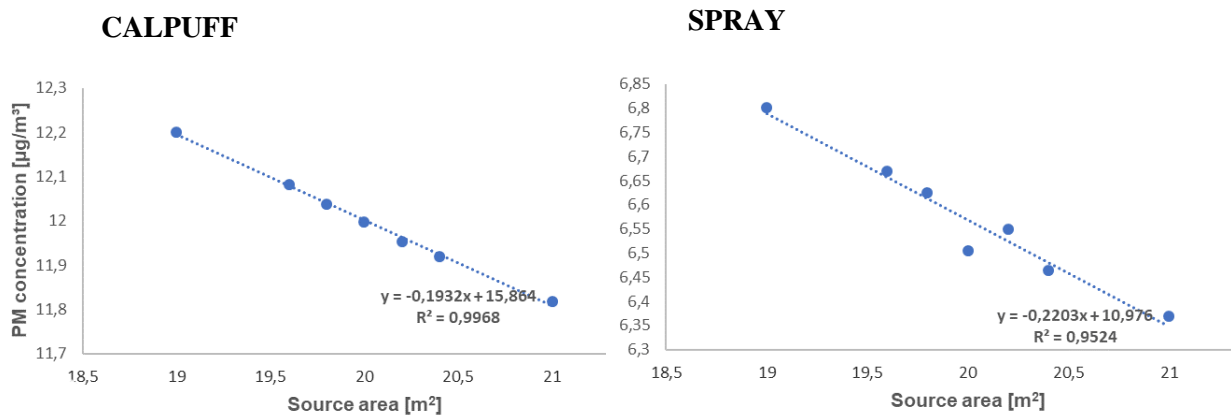


Figure 18. Maximum 1-hour PM concentration as a function of the source area predicted by CALPUFF model (left) and by the SPRAY model (right) on receptors located at 3000 m from the source

Concentrations predicted by CALPUFF and SPRAY, on a receptor located at 5000 m from the source, at different source areas

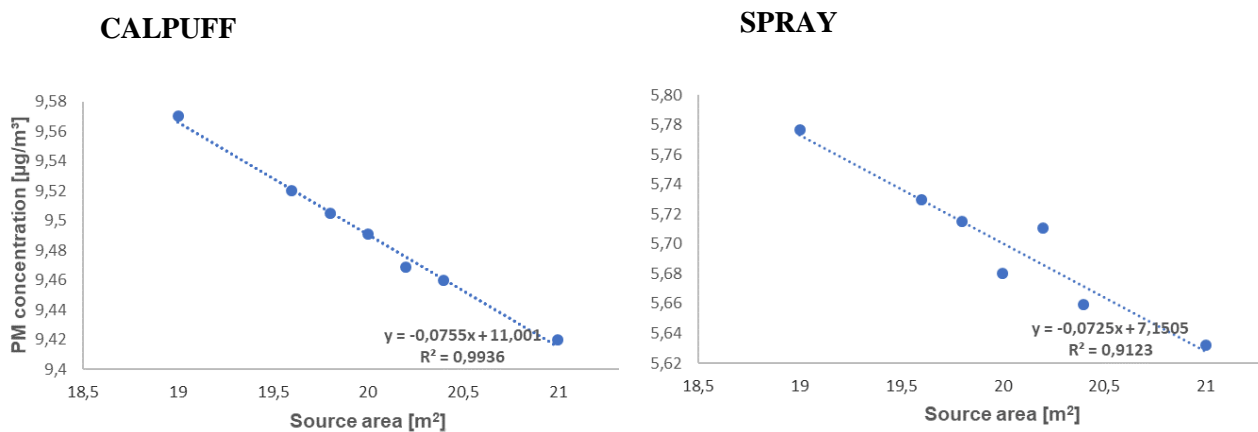


Figure 19. Maximum 1-hour PM concentration as a function of the source area predicted by CALPUFF model (left) and by the SPRAY model (right) on receptors located at 5000 m from the source

Concentrations predicted by CALPUFF and SPRAY, on a receptor located at 7000 m from the source, at different source areas.

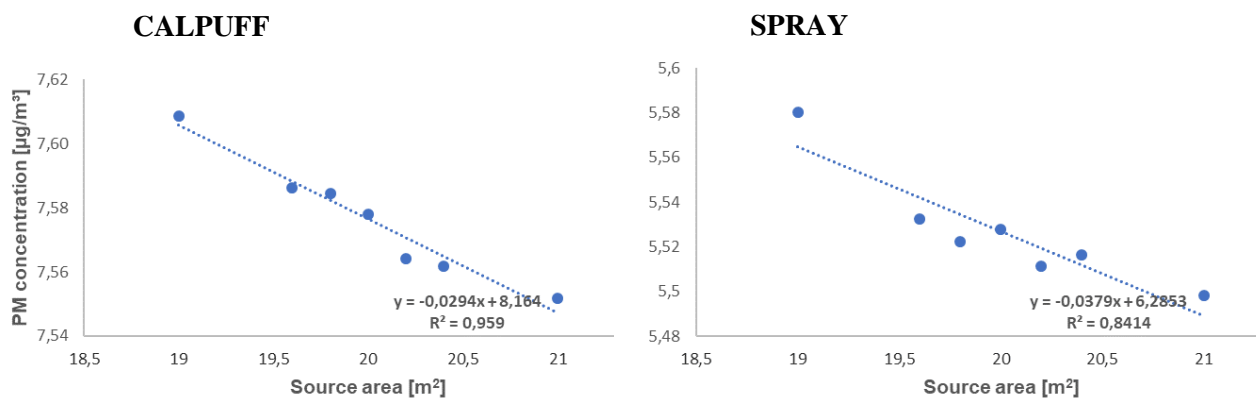


Figure 20. Maximum 1-hour PM concentration as a function of the source area predicted by CALPUFF model (left) and by the SPRAY model (right) on receptors located at 7000 m from the source

SUPPLEMENTARY MATERIAL S6: A SENSITIVITY ANALYSIS APPLIED TO SPRAY AND CALPUFF MODELS WHEN SIMULATING DISPERSION FROM INDUSTRIAL FIRES

Francesca Tagliaferri, Marzio Invernizzi, Laura Capelli

Discussion on the effect of wind field on plume distortion

These maps show that, in the vicinity of the source, the plumes direction remains practically unchanged whereas, at large distances, the wind effect results in a major plume deviation.

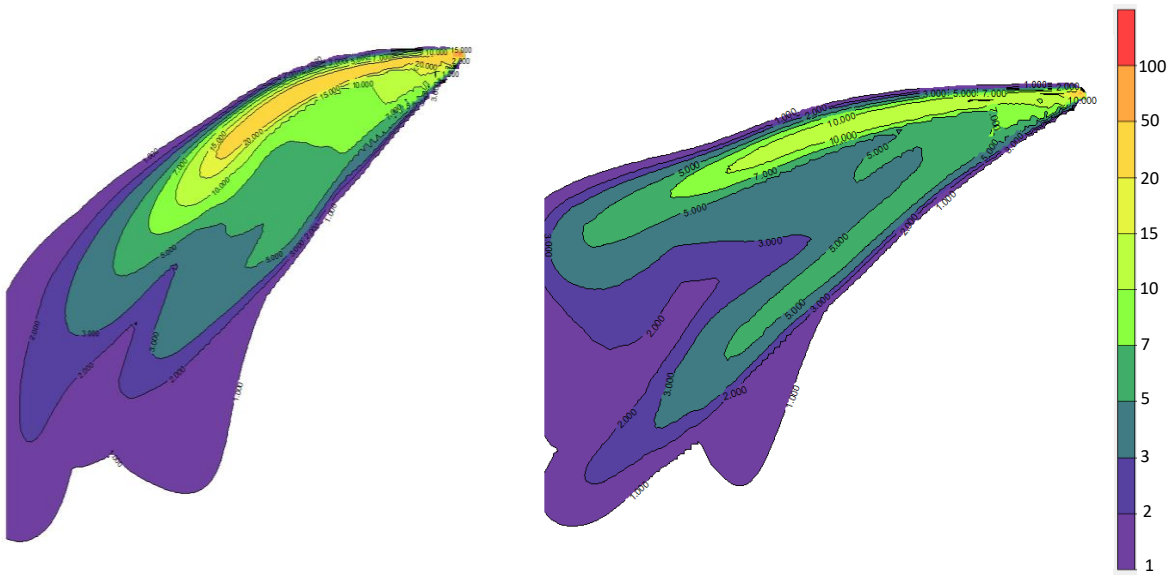


Figure 21. Maximum ground level concentration maps of PM resulting from CALPUFF base scenario (left) and CALPUFF A1 scenario (right)